Study of $e^+e^- \to p\bar{p}$ near threshold and improved TOF reconstruction of antineutron at BSIII

Hailin Song (宋海林)

Supervisor: Qipeng Hu, Xiaorong Zhou

Thesis Proposal Talk

University of Science and Technology of China

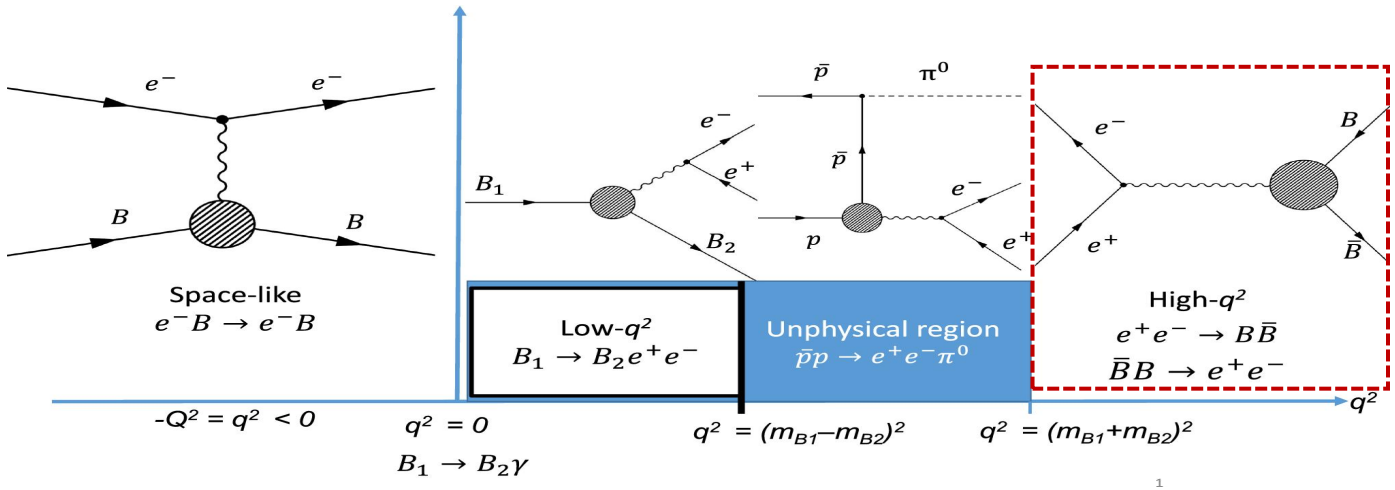
Oct. 13th, 2026

Outline

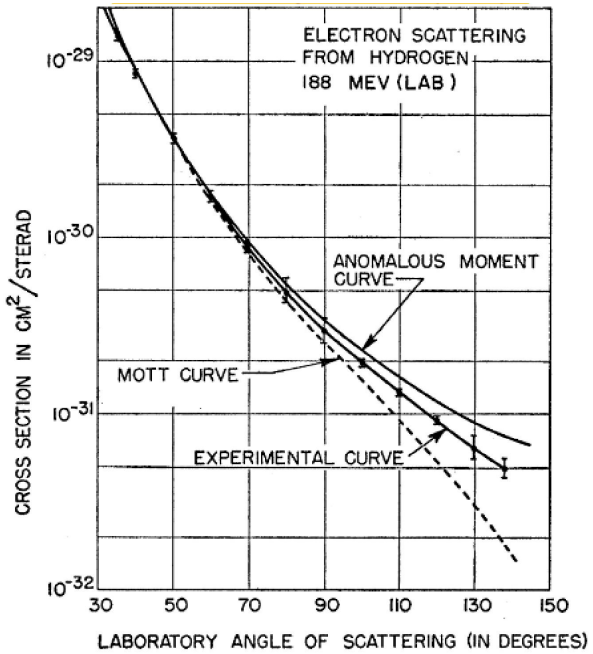
- **Introduction**
- **Current Research Overview**
  - Study of $e^+e^- \to p\bar{p}$ near threshold
  - Improved TOF reconstruction for antineutron at BESIII
- **Summary and Prospects**

Introduction

- Hadrons are **not point-like** particles.
- Electromagnetic Form Factors (EMFFs) are **fundamental properties** of baryons.
  - Connected to **charge and current distributions**.
  - Crucial testing ground for theoretical models of **hadron structure**.



Nobel Prize in 1961
Rev. Mod. Phys. 30, 482 (1958)



Reveals the internal structure inside the nucleon

Hardonic vertex:

$$\Gamma^{\mu}(q) = \gamma_{\mu}F_1(q^2) + \frac{i\sigma_{\mu\nu}q^{\nu}}{2m_p}F_2(q^2)$$

F_1 and F_2 are the Dirac and Pauli FFs

Sachs FFs:

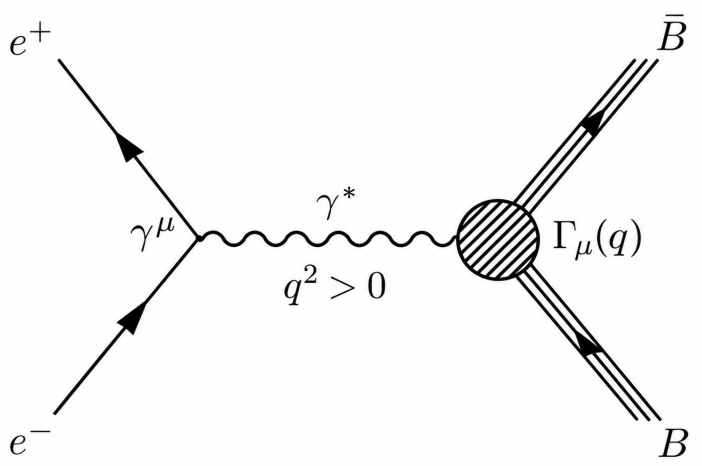
$$G_E(q^2) = F_1(q^2) + \tau\kappa_p F_2(q^2),\ G_M(q^2) = F_1(q^2) + \kappa_p F_2(q^2)$$

Introduction

- The production cross section of $e^+e^- \to B\overline{B}$ (1/2 baryon) is given:

$$\frac{d\sigma_{p\bar{p}}}{d\Omega} = \frac{\alpha^2\beta C}{4s}[|G_M(s)|^2(1+\cos\theta^2) + \frac{1}{\tau}|G_E(s)|^2\sin\theta^2],$$

$$\tau = \frac{s}{4m_p^2}, C = \frac{y}{1-e^{-y}},\ y = \alpha/\beta \text{ (or } C = 1 \text{ for neutral baryon)}$$

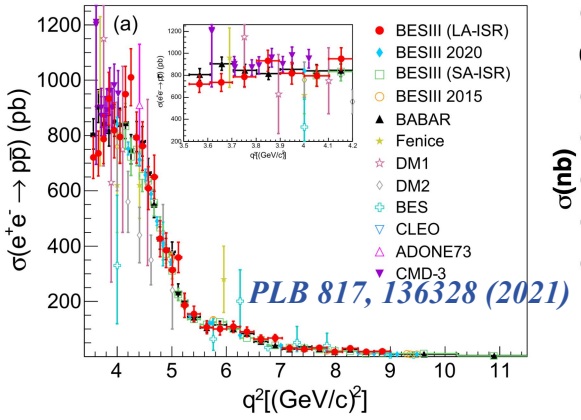


Integrated cross section:

$$\sigma(s) = \frac{4\pi\alpha^2\beta C}{3s}(1+\frac{1}{2\tau})|G_{\text{eff}}|^2,\ |G_{\text{eff}}|^2 = \frac{2\tau|G_M(s)|^2+|G_E(s)|^2}{2\tau+1}$$

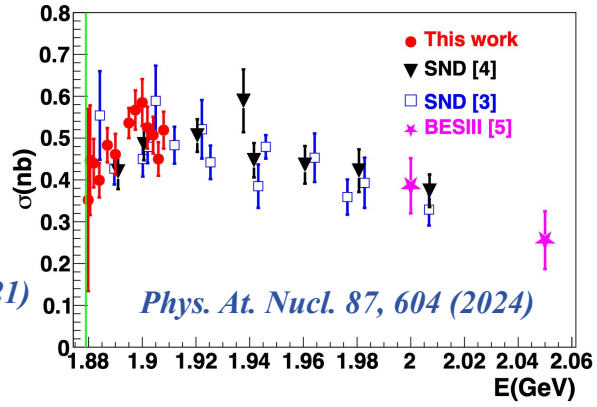
- The **enhancement** of $B\overline{B}$ pair production near threshold:

$e^+e^- \to p\bar{p}$



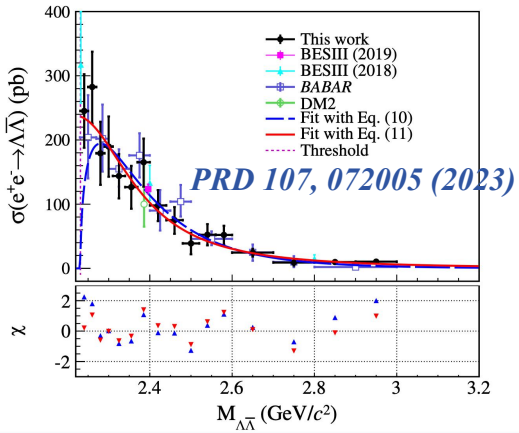
PLB 817, 136328 (2021)

$e^+e^- \to n\bar{n}$



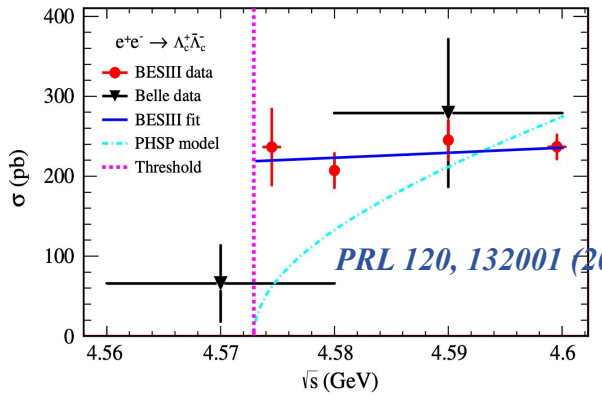
Phys. At. Nucl. 87, 604 (2024)

$e^+e^- \to \Lambda\bar{\Lambda}$



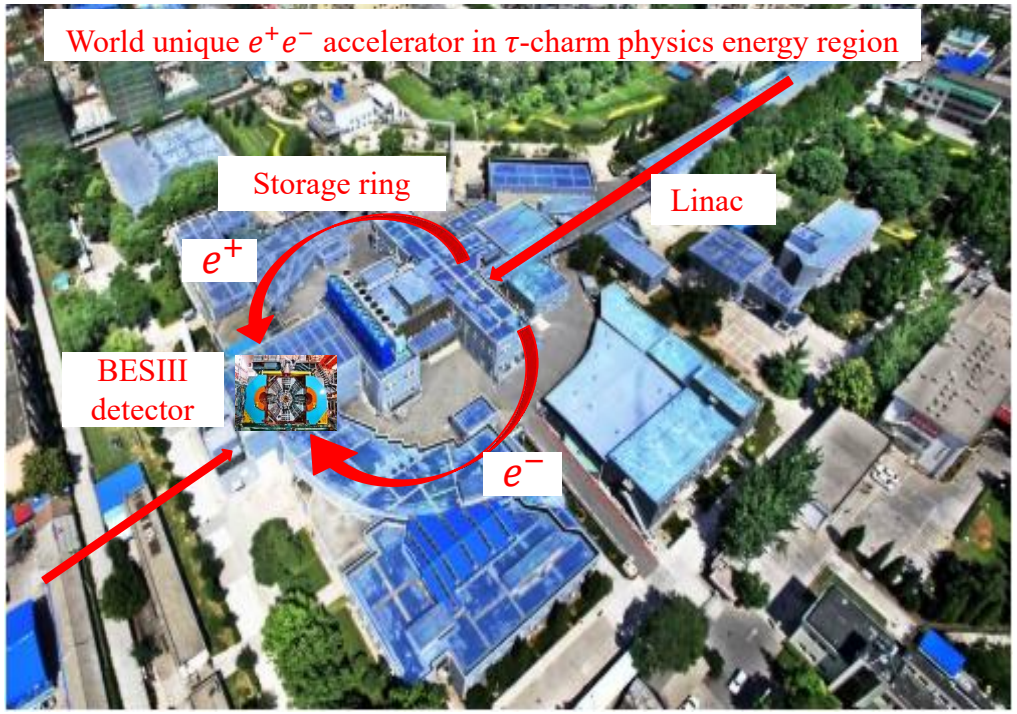
PRD 107, 072005 (2023)

$e^+e^- \to \Lambda_c^+\bar{\Lambda}_c^-$



PRL 120, 132001 (2018)

Introduction to BEPCII and BESIII



Double rings

$E_{cm} = 1.84 - 4.95$ GeV

Peak luminosity @$E_{cm} = 3.773$ GeV:

1.1×10^{33} cm^{-2}s^{-1}

Circumference: 237.53 m

Crossing angle: 2×11 mrad

Electromagnetic Calorimeter

CsI(Tl): L=28 cm

Barrel σ_E=2.5%

Endcap σ_E=5.0%

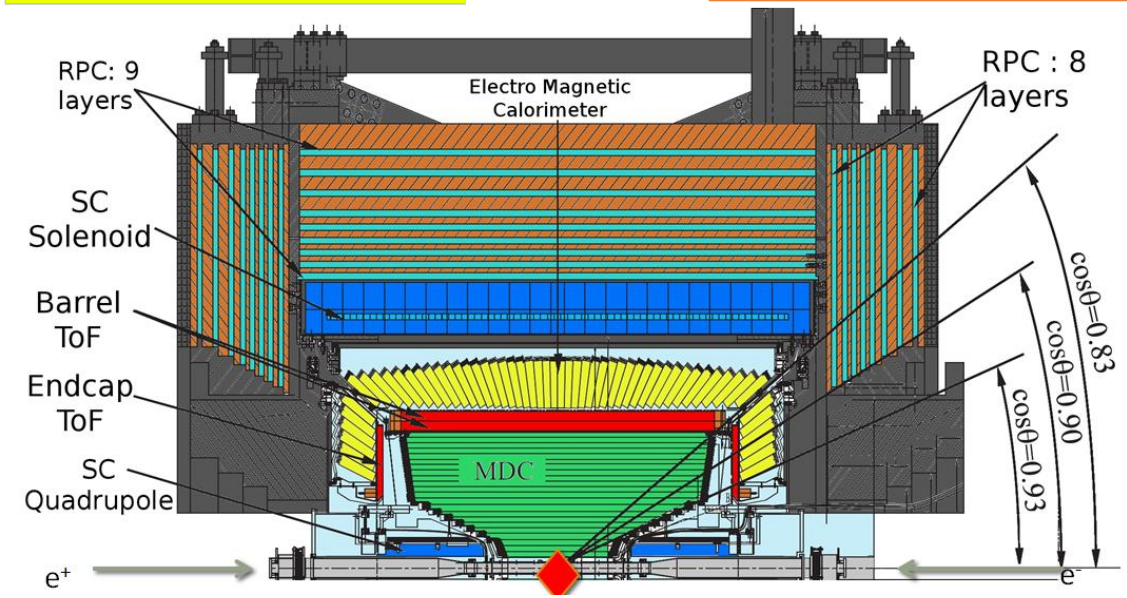
Muon Counter

RPC

Barrel: 9 layers

Endcap: 8 layers

$\sigma_{spatial}$: 1.48 cm



Main Drift Chamber

Small cell, 43 layer

σ_{xy}=130 μm

dE/dx~6%

σ_p/p= 0.5% at 1 GeV

Time Of Flight

Plastic scintillator

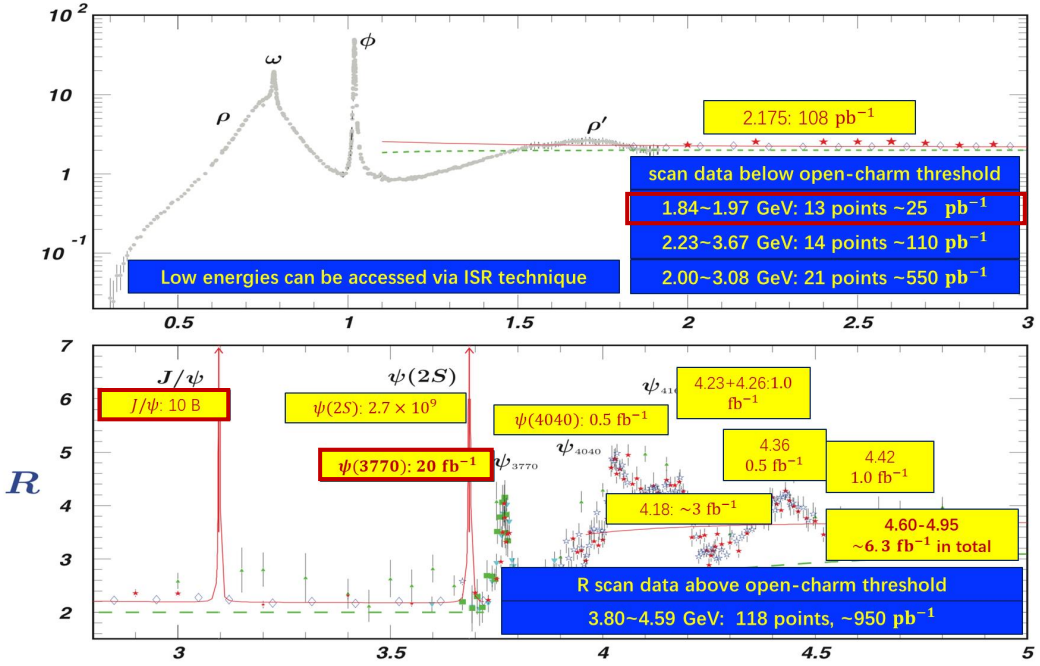
σ_T(barrel): 68 ps

σ_T(endcap): 110 ps

(update to 60 ps with MRPC)

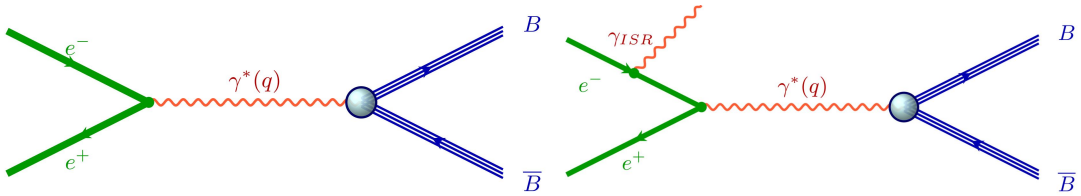
Introduction:
Data Samples at BESIII

- The **advantages** in BESIII:
  - ✓ Large datasets at tau-charm region.
  - ✓ Only experiment enabls both **energy scan and ISR methods**.



BESIII provides **an ideal environment** to measure **inclusive/exclusive hadronic** cross section!

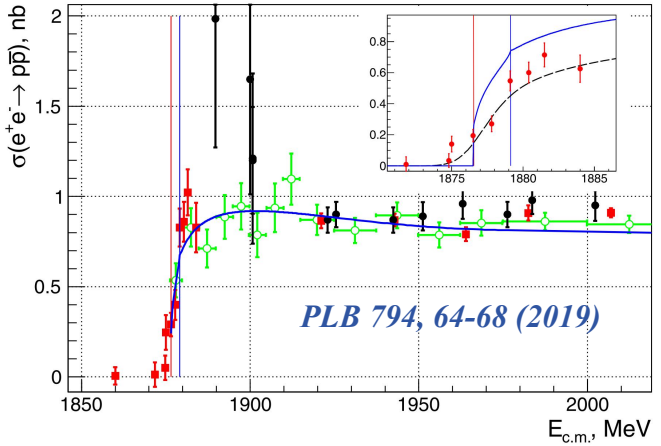
- **Energy Scan Method**:
  - **Well-defined** c.m.energy
  - Very **good** energy resolution
  - **low** background
  - **Discrete values**, leaving gaps without information
- **Initial State Radiation(ISR) Method**:
  - At a fixed c.m.energy $\sqrt{s}$, collecting events **from threshold to $\sqrt{s}$**
  - Systematic uncertainty in a **coherent** way
  - **Large** luminosity needed
  - **Higher** background



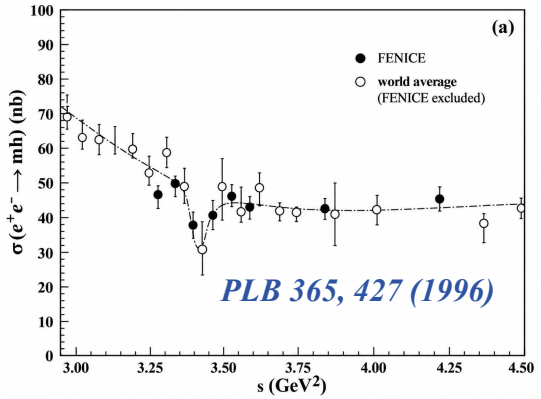
Study of $e^+e^- \to p\bar{p}$ near threshold:

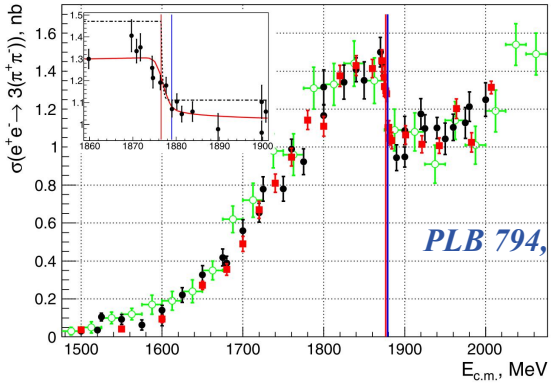
Motivation

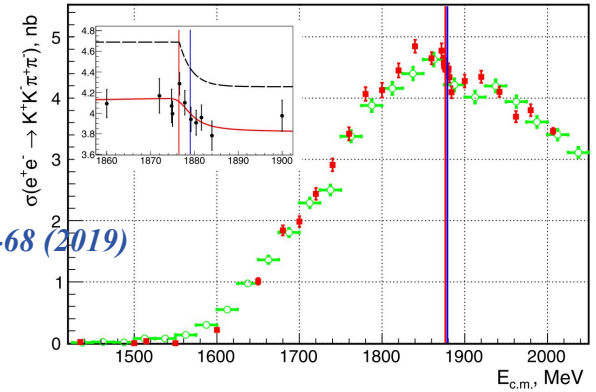
- Anomaly production cross section for $e^+e^- \to p\bar{p}$:
  - ✓ **very sharp step-like behavior**.
  - ✓ The plateau indicates **anomaly threshold effect**.
  - ✓ Uncertainty is still **large**.



- Anomalous behavior around the $p\bar{p}$ threshold has also been observed in other channels.







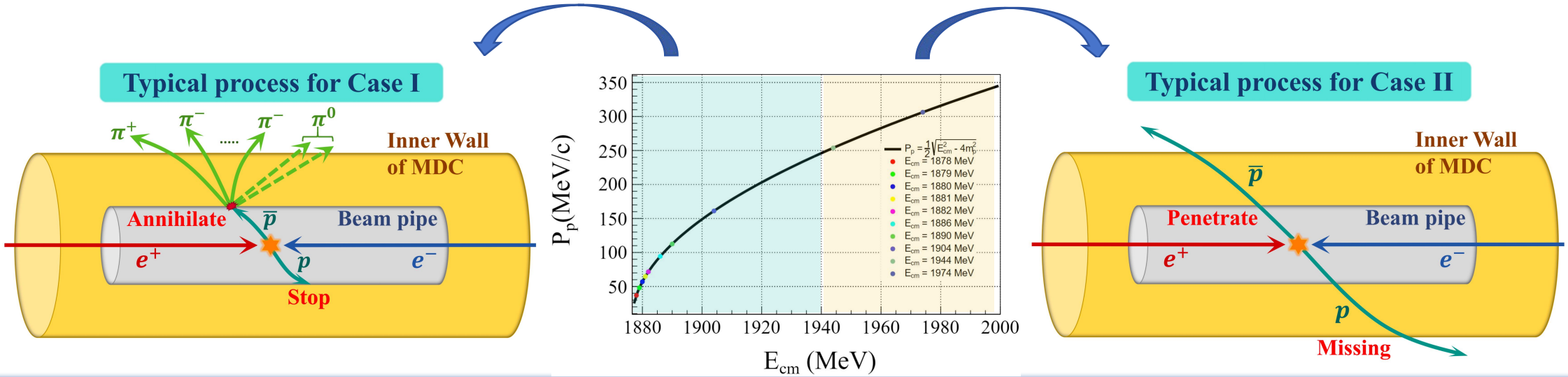
- It seems that there is a **similar origion**? ⇒ **FSI effects**; **bound states**; **meson resonances**...
- BESIII has collected data sets from **1.840 to 1.970 GeV** in 2024, which can be used to study $e^+e^- \to p\bar{p}$ **near threshold** via **scan** method.

Analysis Strategy

◆ **Unconventional** reconstruction method is used, due to low momentum of $p/\bar{p}$.

- Case I (Ecm<1.940 GeV):
  - $p\bar{p}$ are **ionized and stopped** before MDC due to high ionozation energy loss.
  - Reconstruct the $\bar{p}N$ **annihilation point** (R_{xy}, R_z) from secondary particles.
  - Extract signal from the R_{xy} distribution.
- Case II (Ecm≥1.940 GeV):
  - Most protons and antiprotons **can reach MDC** and be detected.
  - **Only detect $\bar{p}$ to improve** efficiency.
  - Extract signal from the **momentum distribution** of antiproton ($P_{\bar{p}}$).

- Data below $p\bar{p}$ threshold can be used to **study the beam-induced** background.



Event Selection

Event Selection for Case I

- **Good Charged Track:**
  $|\cos\theta| \leq 0.93$; $\mathbf{N_{charged} \geq 2}$.
- **Good Photon:**
  $E_{\rm barrel} \geq 25$ MeV ($|\cos\theta| < 0.80$); $E_{\rm endcap} \geq 50$ MeV ($0.86 < |\cos\theta| < 0.92$); $0 \leq TDC \leq 700$ ns.
- **PID: Only use dedx**
  π: prob(π)>0.001 and prob(π)>prob(p, K, e).
  Require: $\boldsymbol{N_{\pi^+} \geq 1}$ **and** $\boldsymbol{N_{\pi^-} \geq 1}$.
- **Vertexfit:**
  A vertex fit is performed to **all the selected charged tracks**. Interacion points($\boldsymbol{R_{xy}}$, $\boldsymbol{R_z}$) are obtained.

Event Selection for Case II

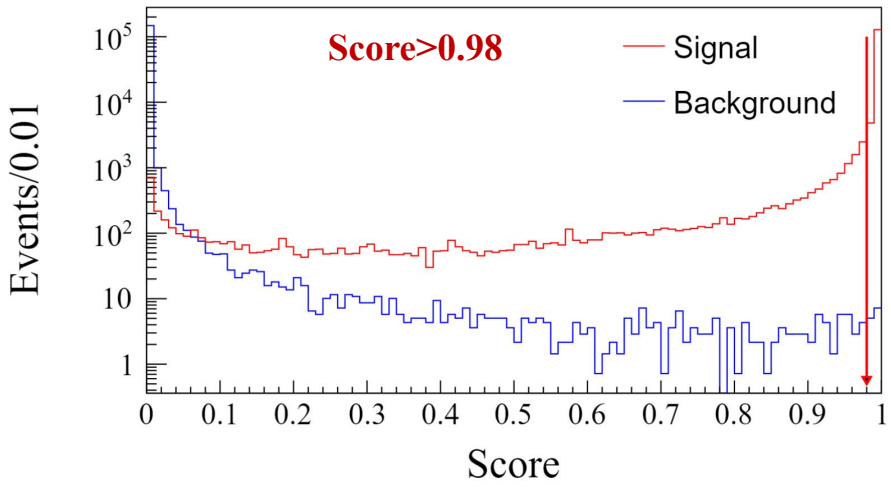
- **Good Charged Track:**
  $|\cos\theta| \leq 0.93$, $|V_{xy}| < 1$ cm, $|V_z| < 10$ cm;
  $\boldsymbol{N_{charged} \geq 1}$.
- **PID: use normPH**
  $\bar{p}$: normPH>(5, 8) for 1943.7 and 1973.5 MeV
  Require: $\boldsymbol{N_{\bar{p}} = 1}$.
- **Further Selection:**
  Momentum window for $\bar{p}$:
  $0.21 < P_{\bar{p}} < 0.28$ GeV/c for 1943.7 MeV
  $0.26 < P_{\bar{p}} < 0.33$ GeV/c for 1973.5 MeV

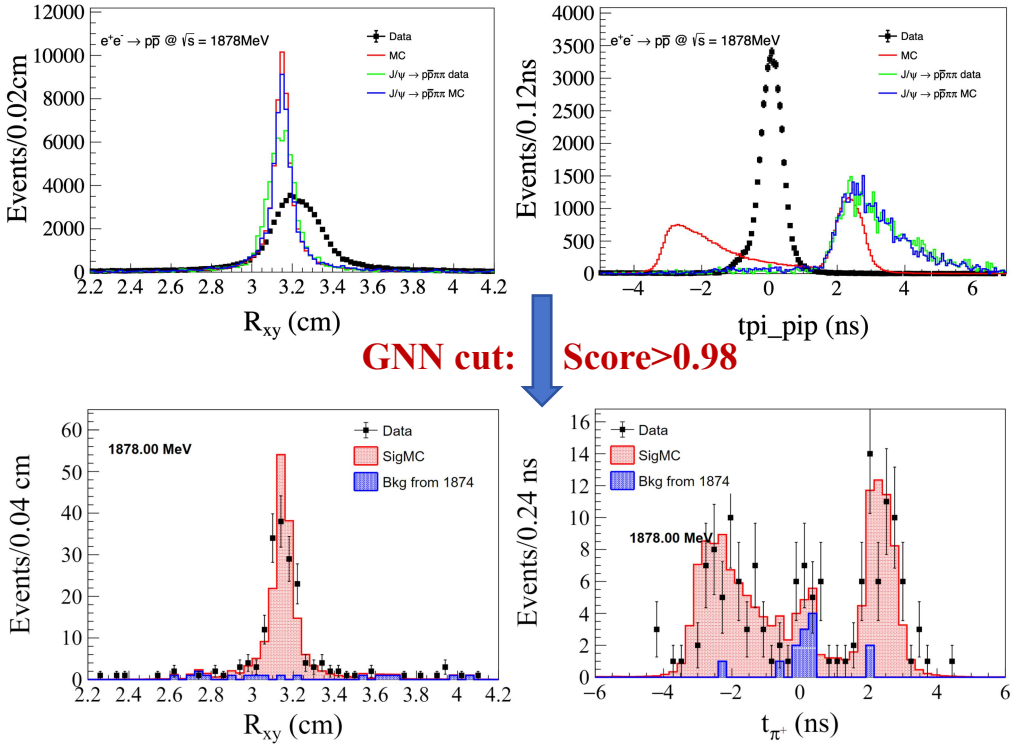
Study of $e^+e^- \to p\bar{p}$ near threshold:
Analysis Challenges

- **High background** after event selection for case I:
  - ➢ High beam background. (**~150:1**)
  - ➢ Overlap with signal peak.

➡ **Machine learning method**:

- ✓ Use a GNN model (**Particle Net**) to supress the background. (**BDT** method as a cross check)
- ✓ Use low level variables for training.



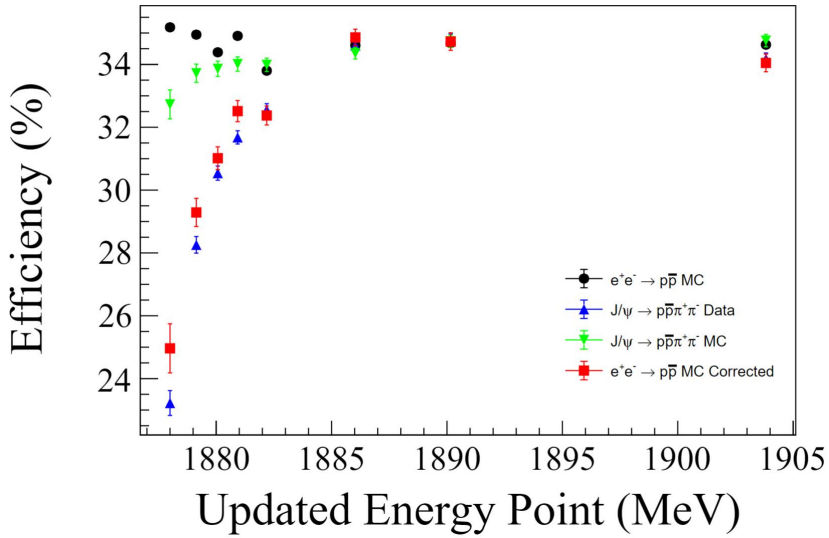


Approximately 90% signal efficiency is achieved with a background rejection exceeding 99.98%.

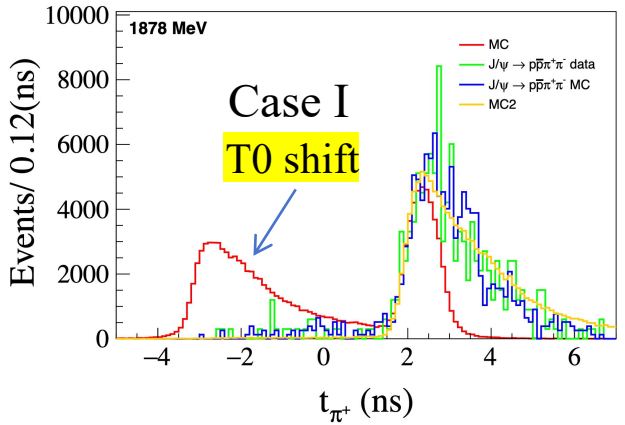
Study of $e^+e^- \to p\bar{p}$ near threshold:
Analysis Challenges

- **Discrepancy** between data and MC:
  - ✓ Use $\bar{p}$ control sample selected from $J/\psi \to p\bar{p}\pi^+\pi^-$.
  - ✓ Compare key variables and evaluate efficiency correction.

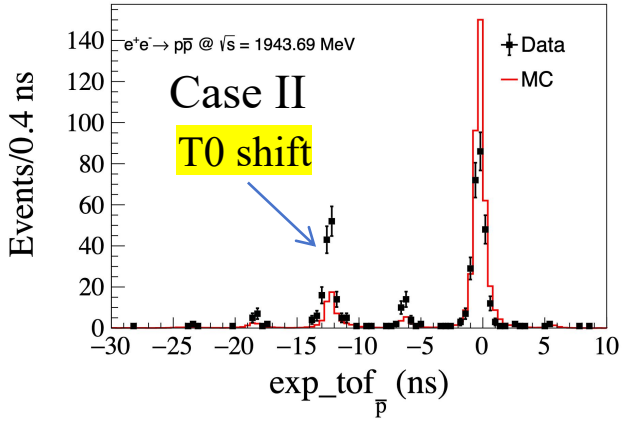
$$\varepsilon_{e^+e^-\to p\bar{p}\ \mathrm{Corr}} = \varepsilon_{e^+e^-\to p\bar{p}\ \mathrm{MC}} \frac{\varepsilon_{J/\psi\to p\bar{p}\pi\pi\ \mathrm{data}}}{\varepsilon_{J/\psi\to p\bar{p}\pi\pi\ \mathrm{MC}}}$$



- **Mismatch of T0** (event start time):
  - ✓ Data and MC are **consistent** in Case I.
  - ✓ Considered as a source of systematic uncertainty in Case II.



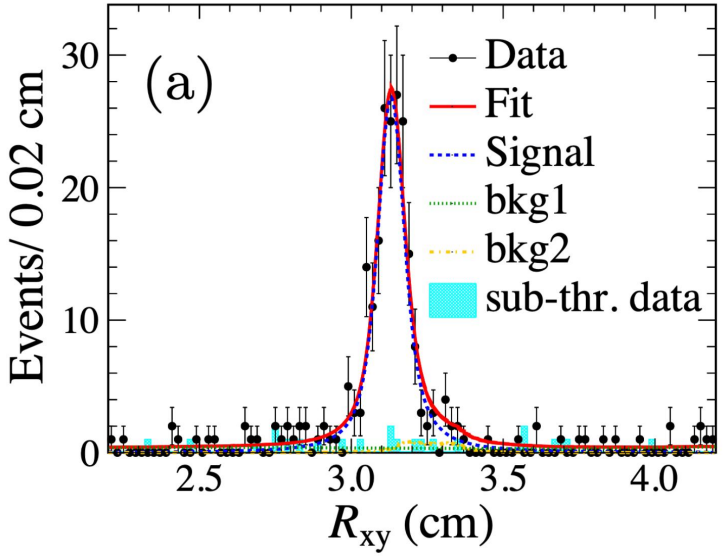
✓ Caused by long fly time of $\bar{p}$ before its annihilation.



✓ Caused by poor T0 algorithm.

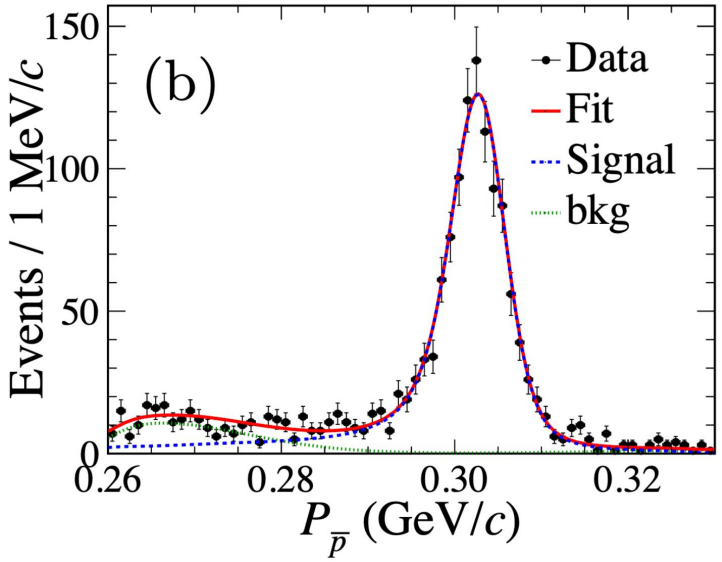
Signal Extraction

- The signal yields are extracted via an unbinned maximum-likelihood fit to R_{xy} or $P_{\bar{p}}$ distribution.
  - Case I at $\sqrt{s} = 1880.9$ MeV:



  - ✓ Total fit = MC shape ⊗ Gaussian (Signal) + 2nd-order Polynomial (bkg1) + $n\bar{n}$ MC shape (bkg2)
  - ✓ Fix $n\bar{n}$ contribution to the data driven estimation.

  - Case II at $\sqrt{s} = 1973.5$ MeV:



  - ✓ Total fit = MC shape ⊗ Gaussian (Signal) + $q\bar{q}$ MC shape ⊗ Gaussian (bkg)

Systematic Uncertainty

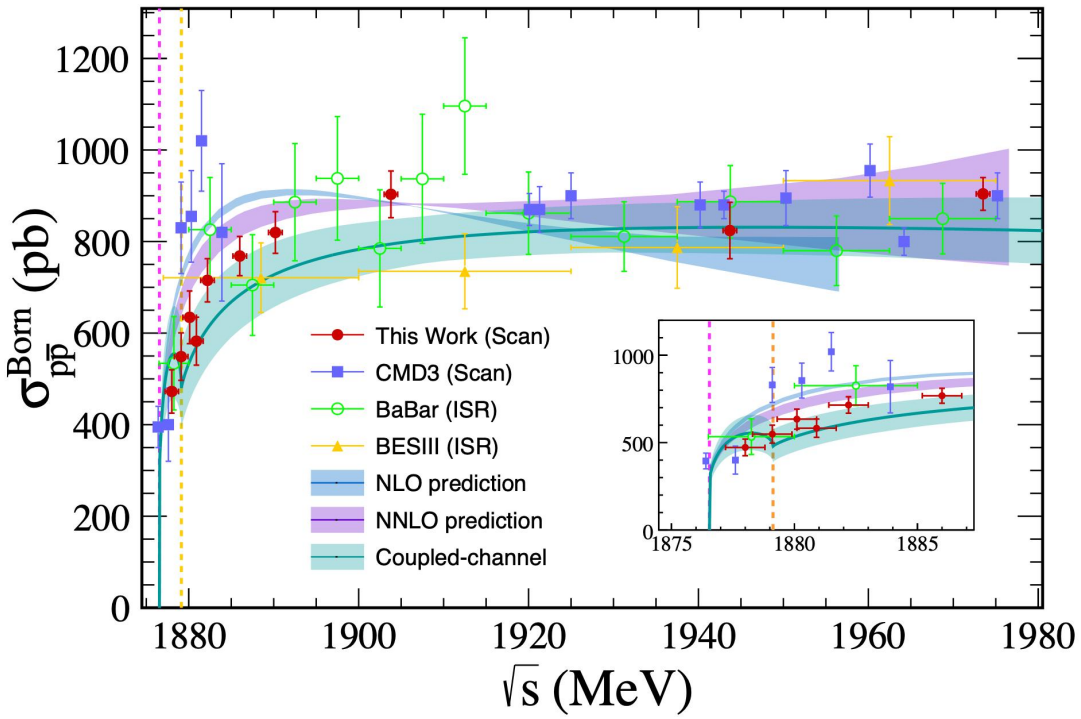
- ✓ All the possible systematic uncertainties are considered for Case I and Case II.
- ✓ The total one calculated by adding all individual contributions in quadrature.
- ✓ The total systematic uncertainties range from **2.2% to 10.7%**.

$\sqrt{s}$ (MeV)	ε corr.	case-related				Fit	MC model	MC stat.	Energy cali.	Lum.	Total
		GNN-related	$n\bar{n}$ bkg	T_0	PID						
1876.0	2.2	8.2	-	-	-	5.4	0.2	0.2	3.5	1.0	10.7
1878.0	2.3	3.7	-	-	-	0.3	0.2	0.2	3.5	1.0	5.7
1879.1	1.4	3.0	1.0	-	-	0.1	0.1	0.2	3.7	1.0	5.1
1880.1	1.0	6.0	1.2	-	-	0.1	0.5	0.2	1.1	1.0	6.4
1880.9	1.0	4.2	1.1	-	-	0.5	0.1	0.2	0.6	1.0	4.7
1882.2	0.9	2.6	0.7	-	-	0.1	0.1	0.2	0.2	1.0	3.1
1886.0	0.7	1.5	0.4	-	-	0.9	0.2	0.2	0.4	1.0	2.2
1890.2	0.9	2.3	0.4	-	-	0.4	0.4	0.2	0.4	1.0	2.8
1903.8	0.9	3.0	0.2	-	-	0.5	0.3	0.2	0.1	1.0	3.4
1943.7	0.2	-	-	5.0	3.1	2.2	0.8	0.1	0.7	1.0	6.5
1973.5	0.1	-	-	1.4	1.6	0.9	0.8	0.1	0.2	1.0	2.7

Study of $e^+e^- \to p\bar{p}$ near threshold:
Analysis Results

- The Born cross section has been measured with **unprecedented precision** near threshold.
  - ✓ A pronounced **threshold enhancement** is observed.
  - ✓ Compared with the CMD-3 results, the BESIII cross section **rises more gradually**.
  - ✓ Provide **precise constraints** on different theoretical models.

$$\sigma_{p\bar{p}}^{obs} = \frac{N_{obs} - N_{bkg}}{L * \varepsilon_{cor} * (1+\delta)}$$



$\sqrt{s}$ (MeV)	$N_{\rm sig}$	$\mathcal{L}$ (pb^{-1})	$\varepsilon_{\rm cor}$(%)	$(1+\delta)$	$\sigma_{\rm Born}$ (pb)
1876.0	34 ± 7	2.014	24.7	-	$68 \pm 17 \pm 7$
1878.0	170 ± 14	2.019	25.5	0.70	$473 \pm 39 \pm 27$
1879.1	177 ± 14	1.485	29.8	0.73	$548 \pm 43 \pm 28$
1880.1	295 ± 19	2.035	30.8	0.74	$634 \pm 41 \pm 40$
1880.9	195 ± 15	1.341	33.1	0.75	$582 \pm 45 \pm 27$
1882.2	360 ± 21	2.021	32.5	0.77	$715 \pm 42 \pm 22$
1886.0	431 ± 22	2.033	34.7	0.80	$768 \pm 39 \pm 17$
1890.2	482 ± 23	2.031	35.5	0.82	$820 \pm 39 \pm 23$
1903.8	534 ± 24	2.022	34.2	0.85	$903 \pm 41 \pm 31$
1943.7	817 ± 31	2.040	53.6	0.91	$824 \pm 31 \pm 53$
1973.5	1287 ± 38	2.229	69.0	0.93	$904 \pm 27 \pm 24$

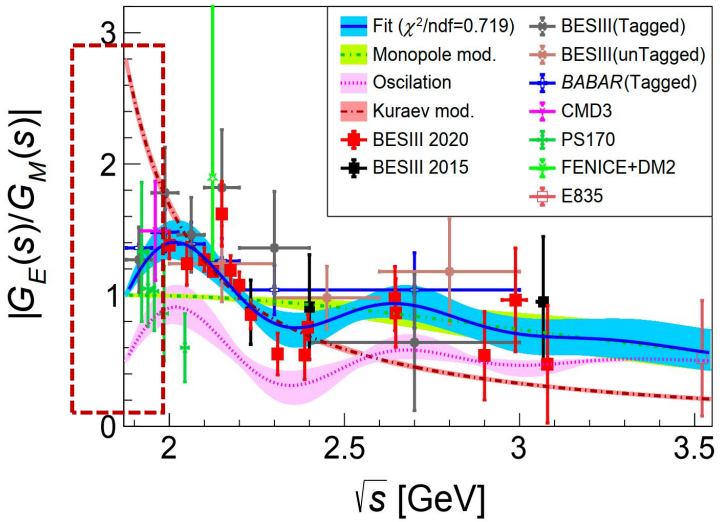
Study of $e^+e^- \to p\bar{p}$ near threshold:
Move to $|G_E/G_M|$ Measurement

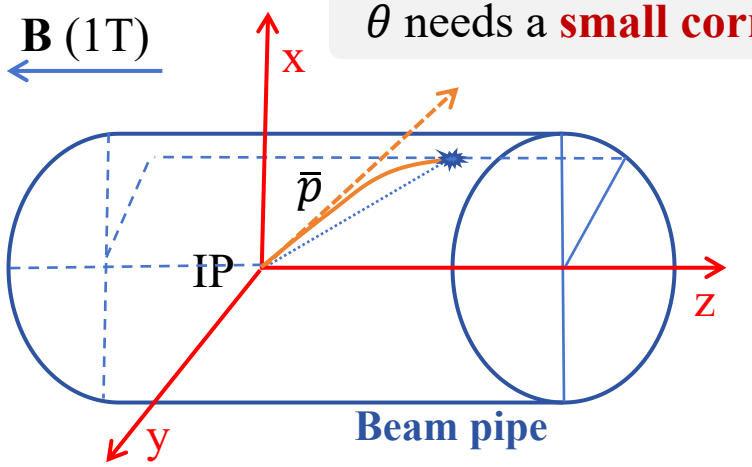
- $|G_E/G_M|$ has been measured across a borad $\sqrt{s}$ range.
- **Damped oscillation** distribution.
- Results near the threshold are **very scarce.**

✓ Angular analysis to exact $|G_E/G_M|$.

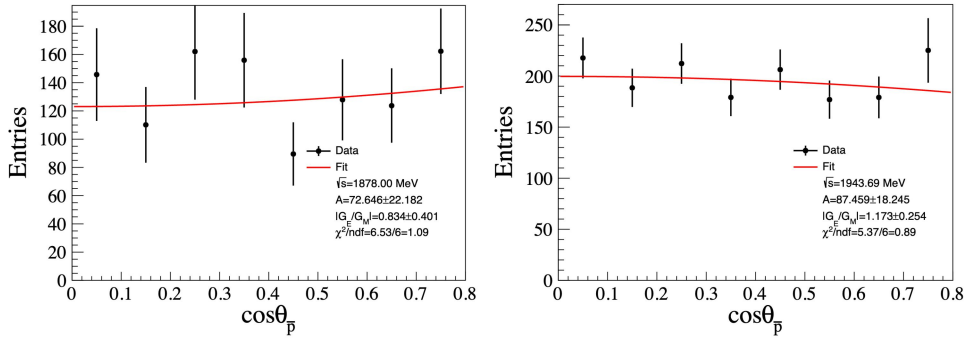
$$\frac{dN}{\varepsilon(1+\delta)\times dcos\theta} = \frac{\mathcal{L}\hbar c\pi\alpha^2\beta C}{2s}|G_M(s)|^2[(1+\cos\theta^2)+\frac{1}{\tau}\frac{|G_E(s)|^2}{|G_M(s)|^2}\sin\theta^2],$$

$$\tau = \frac{s}{4m_p^2}, C = \frac{y}{1-e^{-y}},\ y = \pi/\beta$$





θ needs a **small correction**

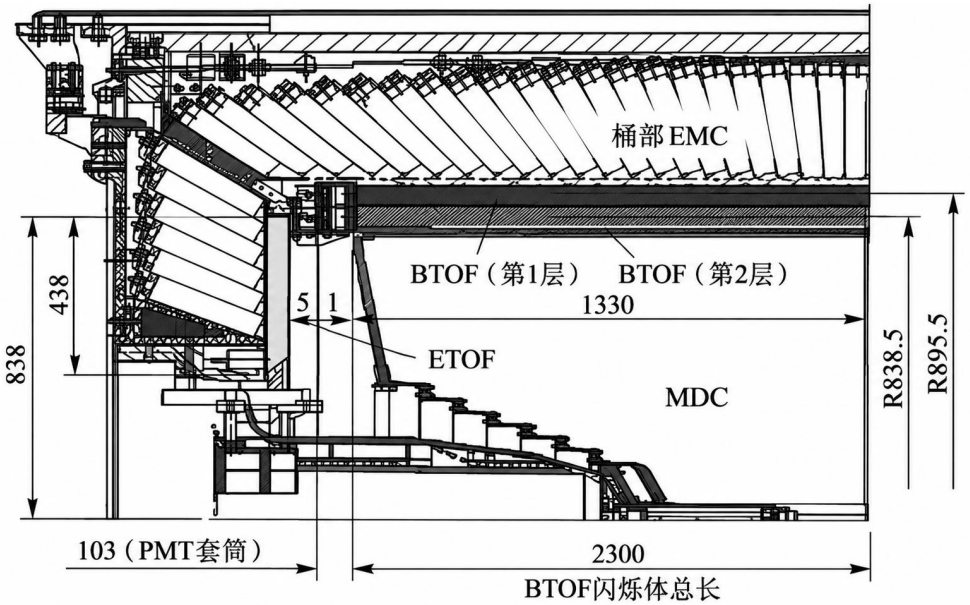


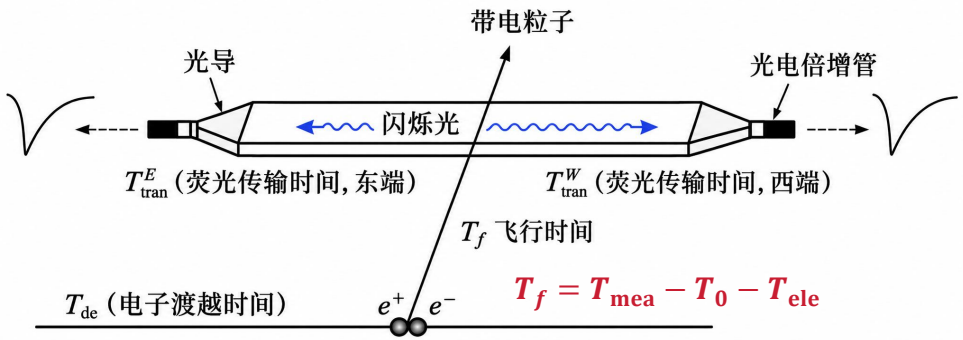
- Corrections for efficiency, ISR factor need further study.
- Systematic uncertainty.

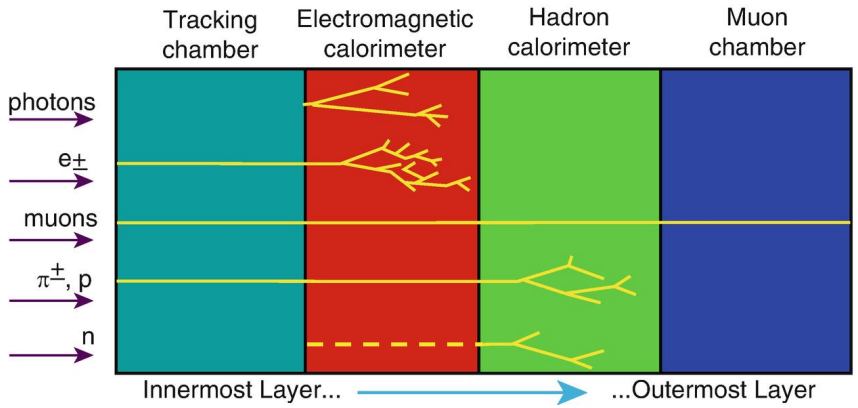
Improved TOF Reconstruction for Antineutron at BESIII:

Motivation

- At BESIII, TOF measurements yield the velocity of a charged particle to do particle identification.
- The neutral particle can also produce light in scintillators, which can be employed to measure the time of flight.
- The efficiency of TOF reconstruction for neutral particles is **(very) low**.
- TOF reconstruction of neutral tracks may be highly **beneficial for some special decay channels**, such as $e^+e^- \to \gamma_{\rm isr} n\bar{n}$, $\bar{\Sigma}^+ \to \bar{n}e^+\nu_e$ and so on.







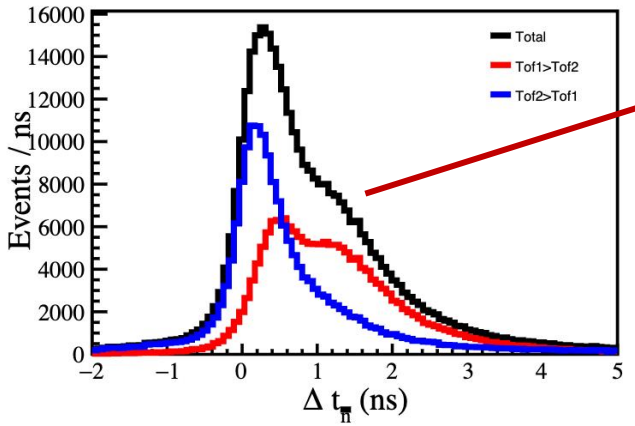
Improved TOF Reconstruction for Antineutron at BESIII:

Method of TOF Reconstruction

- Matching the EMC showers to the TOF hits and using standard TOF calibrations.

  ✓ $\Delta t_{\bar{n}} = t_{\mathrm{mea}} - t_0 - t_{\mathrm{exp}(\bar{n})}$
  - t_{mea} is the matched tof hit time.
  - t_0 is the event start time.
  - $t_{\mathrm{exp}(\bar{n})} = t_{\mathrm{exp}(\gamma)}/\beta_{\bar{n}}$.
  - $t_{\mathrm{exp}(\gamma)} = L_{\mathrm{exp}}/c$.

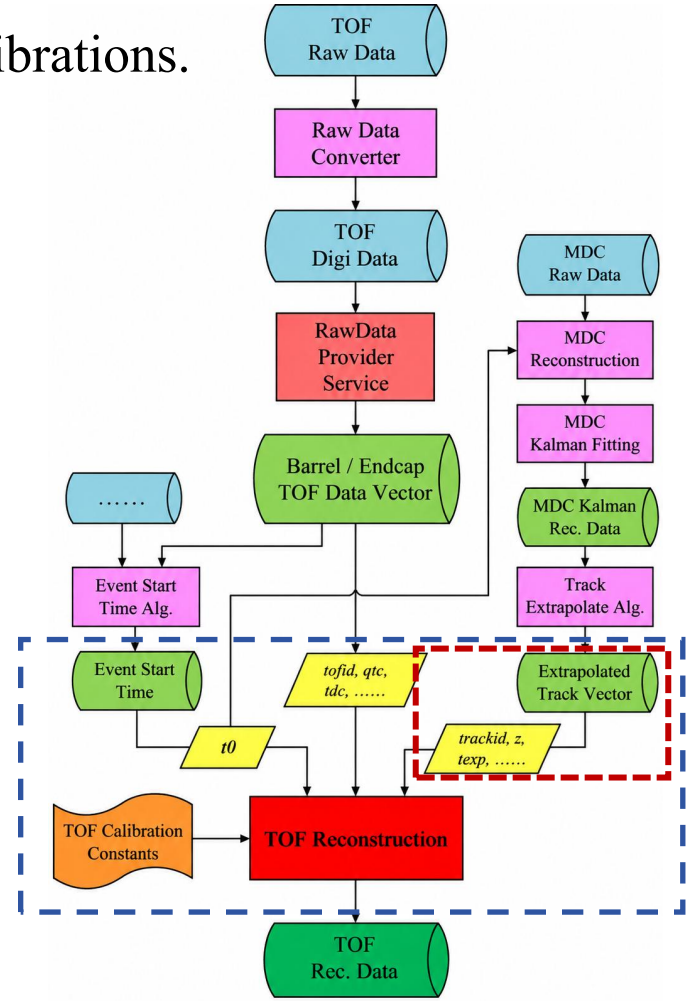
- $\bar{n}$ samples selected from $J/\psi \to p\bar{n}\pi^-$ are used to study the TOF reconstruction method.



Some strange shifts

How to understand?

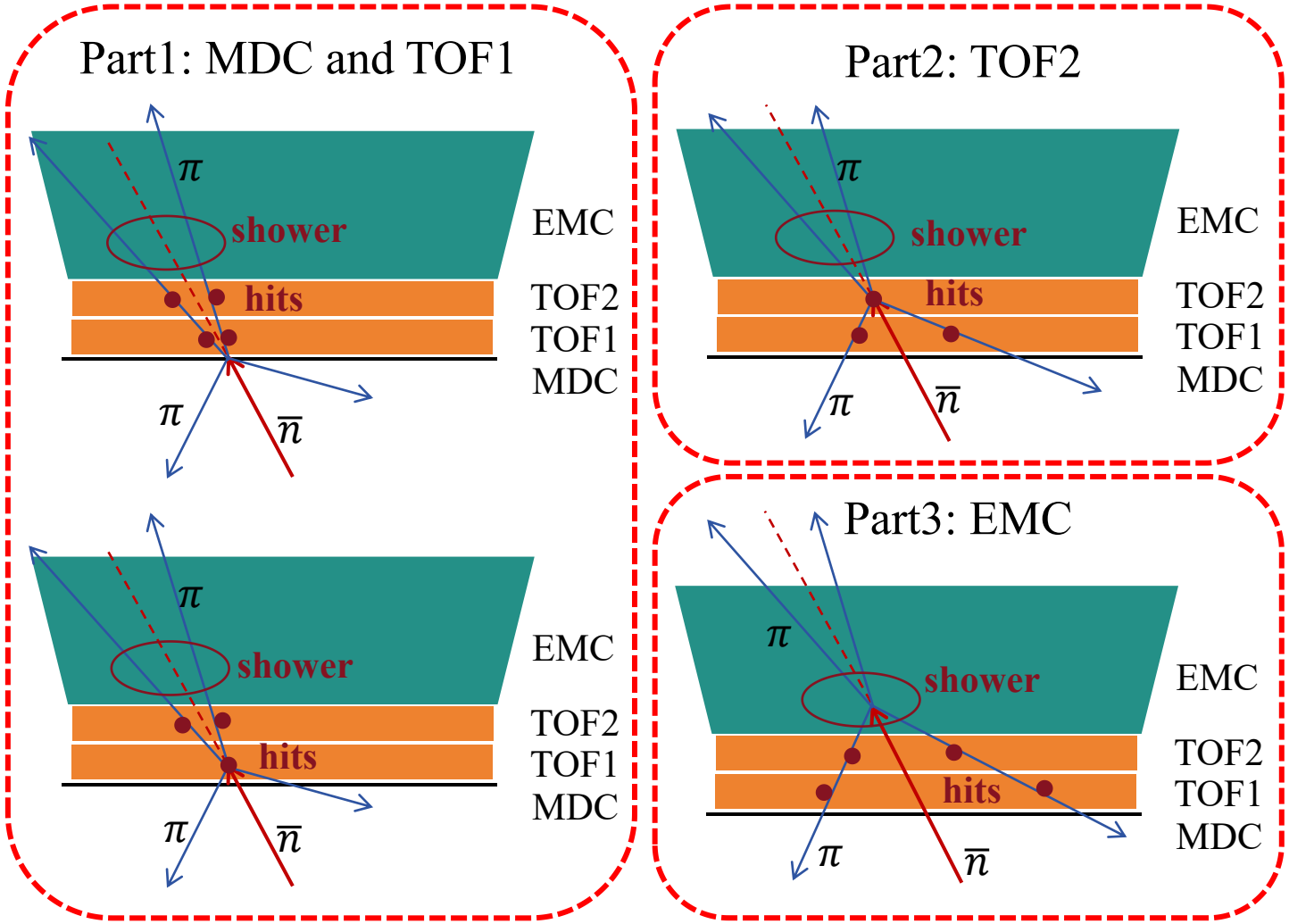
Perform calibration

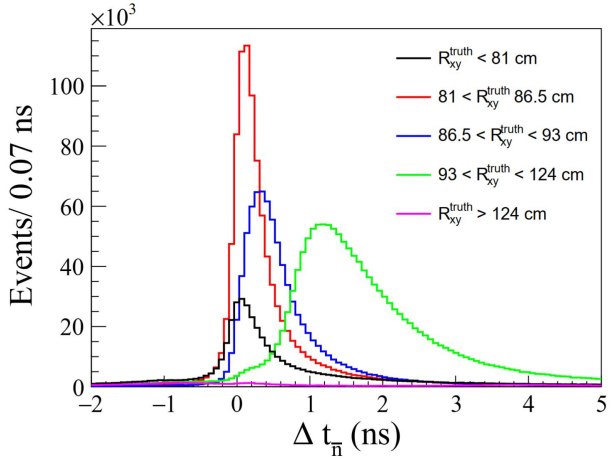


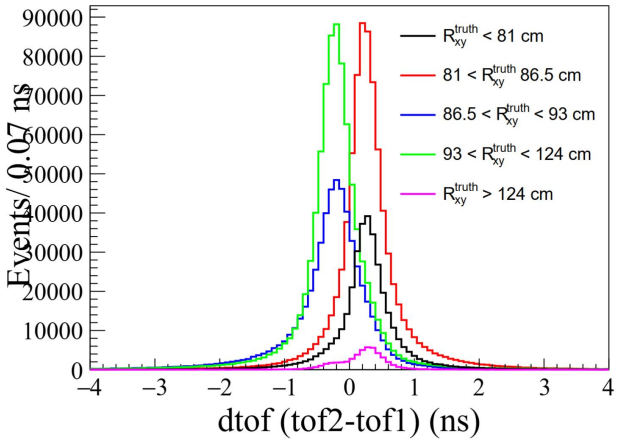
Flow chart of TOF reconstruction for charged tracks

Improved TOF Reconstruction for Antineutron at BESIII:
Study $\Delta t_{\bar{n}}$

- Study $\Delta t_{\bar{n}}$ **by MC**, highly related to R_{xy}^{truth} and dtof (tof2-tof1).

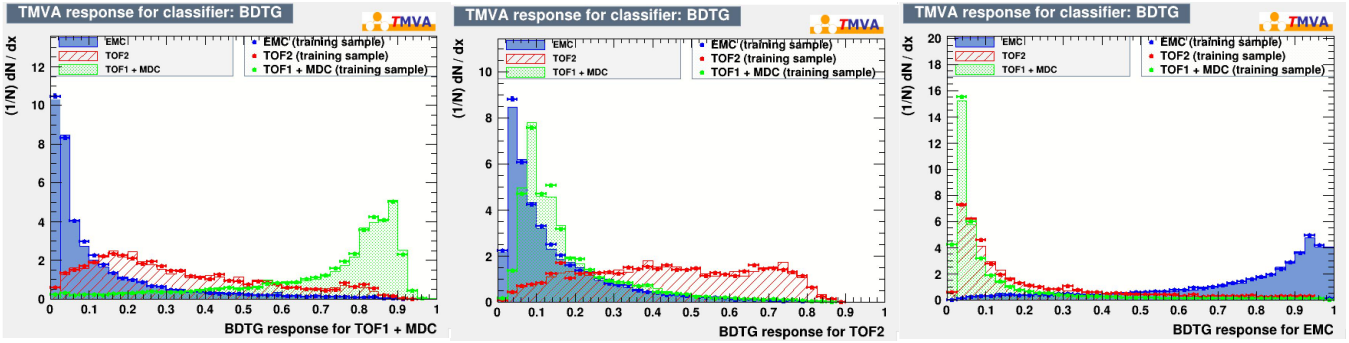




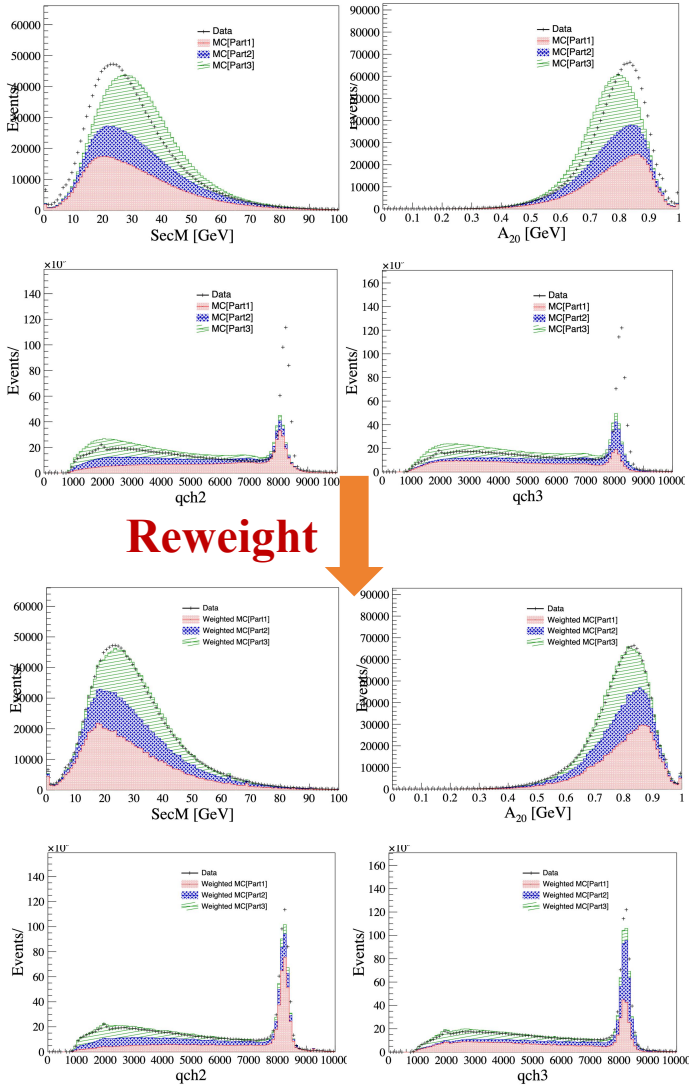


Improved TOF Reconstruction for Antineutron at BESIII:
Classification

- How to **distinguish** these three parts in Data?
  - ✓ Using **shower and TOF infos** to training a BDTG model to classify these three parts.
  - ✓ Only can be trained by MC sample.
  - ✓ Reduce the data/mc difference by **reweight** (XGBoost).



		Data [%] Ratio	MC [%] Ratio/Purity/Eff.
BDTG Classification	Part1	49.6	49.5/75.1/84.3
	Part2	21.9	18.3/70.0/48.0
	Part3	28.5	32.2/69.9/77.2



Improved TOF Reconstruction for Antineutron at BESIII:
Calibration

- The $\bar{n}$ sample are divided into three subsets via BDT classification, and the calibration correction for $\Delta t_{\bar{n}}$ is performed separately for each subset.

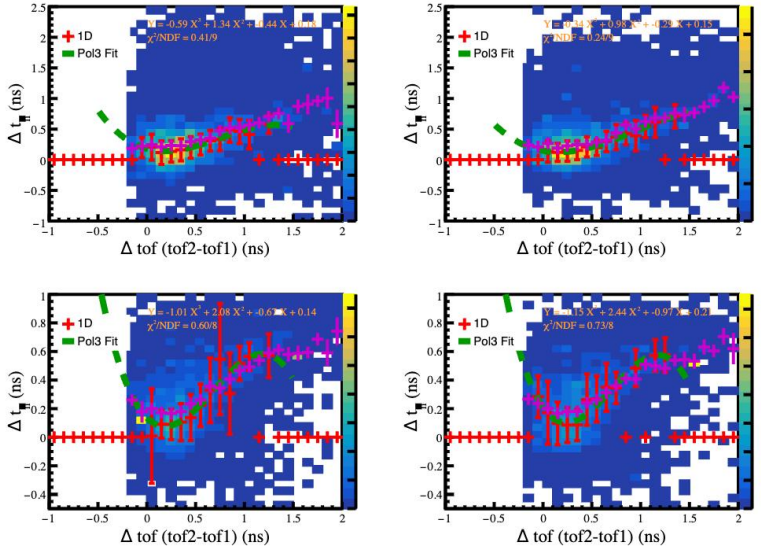
- $\Delta t_{\bar{n}} = t_{\mathrm{mea}} - t_0 - t_{\mathrm{exp}(\bar{n})}$
  - ✓ Introduce $t_{\mathrm{cali}}^{\mathrm{data/MC}}$ to make $\Delta t_{\bar{n}}$ to be 0.

$$t_{\mathrm{exp}(\bar{n})} = t_{\mathrm{mea}} - t_0 - t_{\mathrm{cali}}^{\mathrm{data/MC}}$$

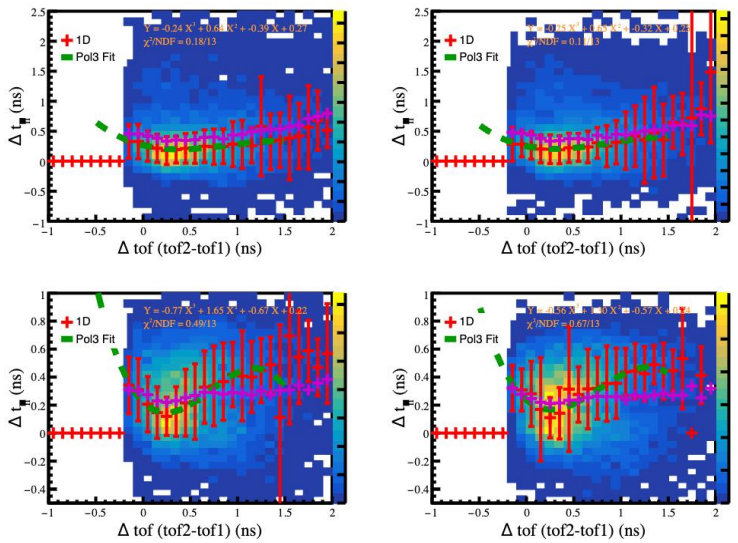
$$\beta_{\bar{n}} = \frac{t_{\mathrm{exp}(\gamma)}}{t_{\mathrm{exp}(\bar{n})}} \rightarrow P_{\bar{n}}^{\mathrm{rec}}$$

- 2D calibration (slice on dtof and dtg):

MC



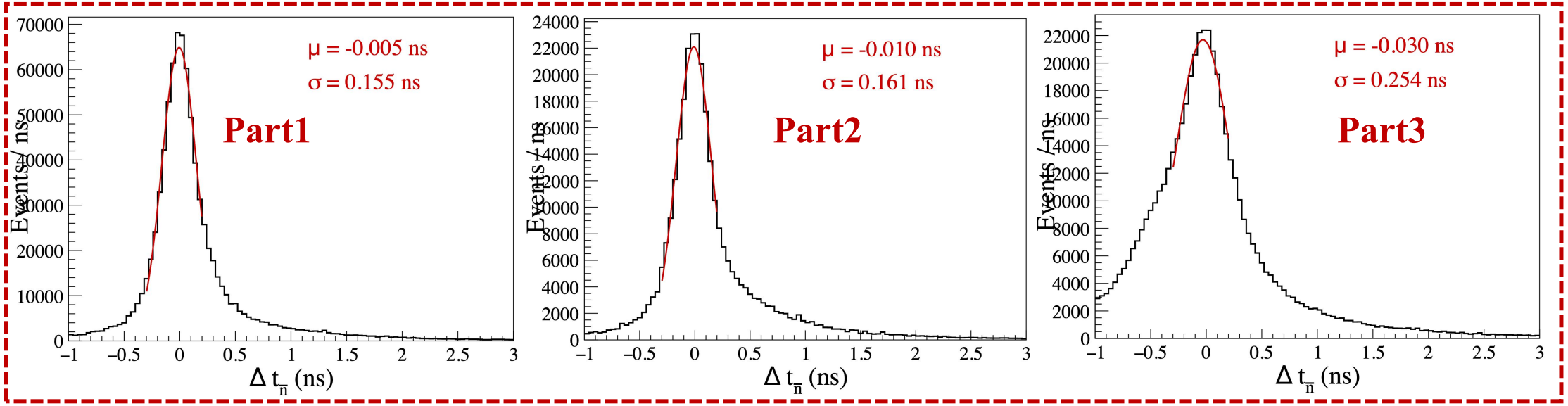
Data



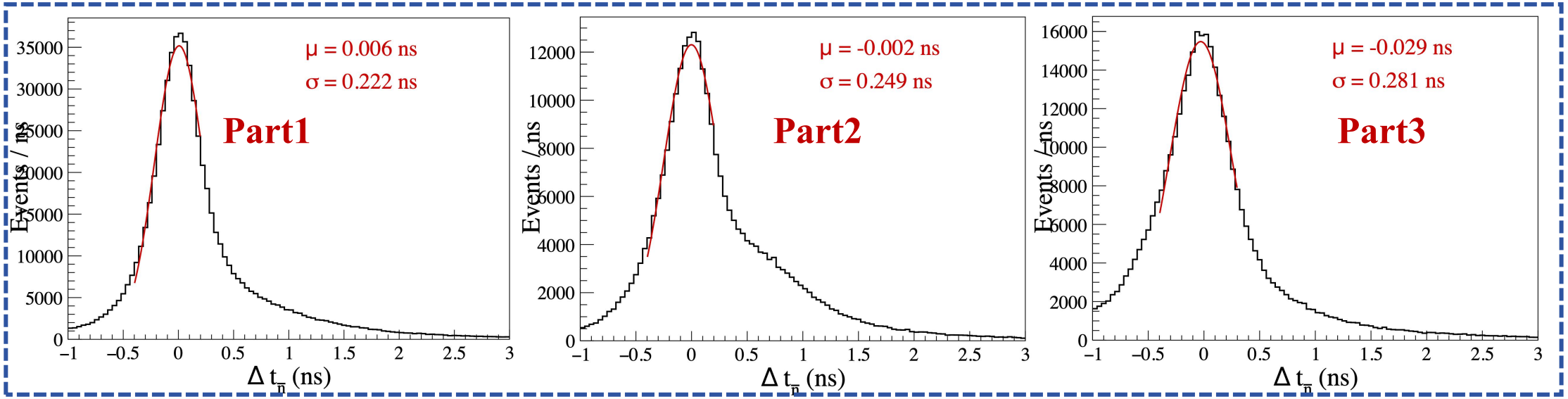
Improved TOF Reconstruction for Antineutron at BESIII:

Results

✓ MC

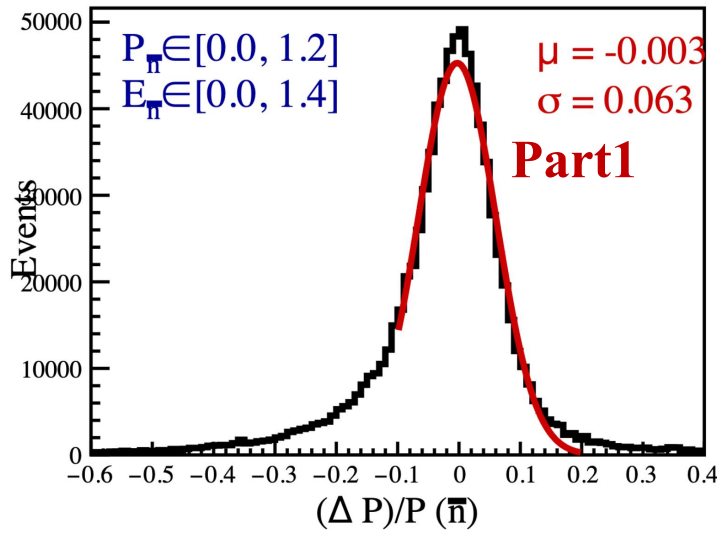


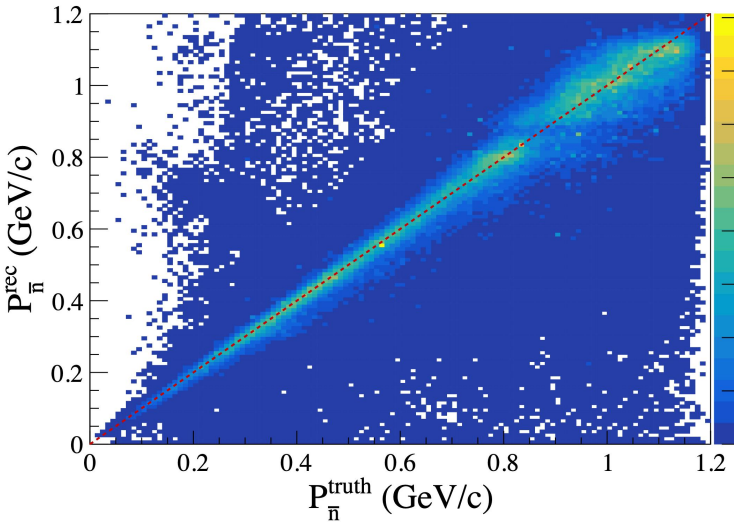
✓ Data

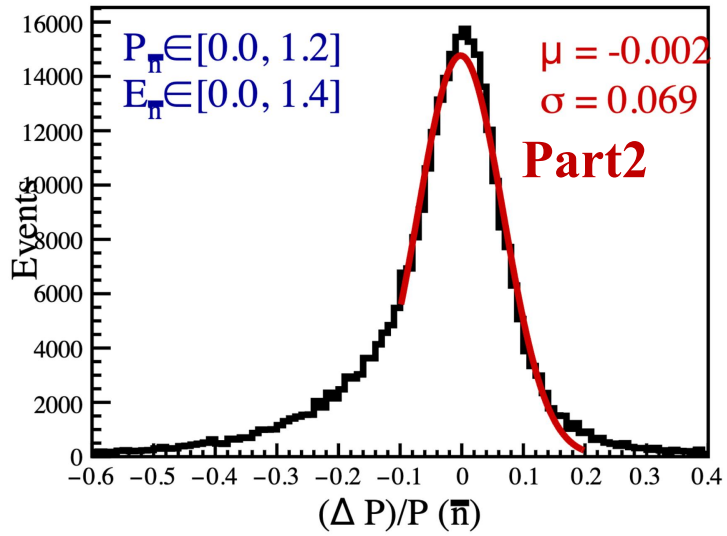


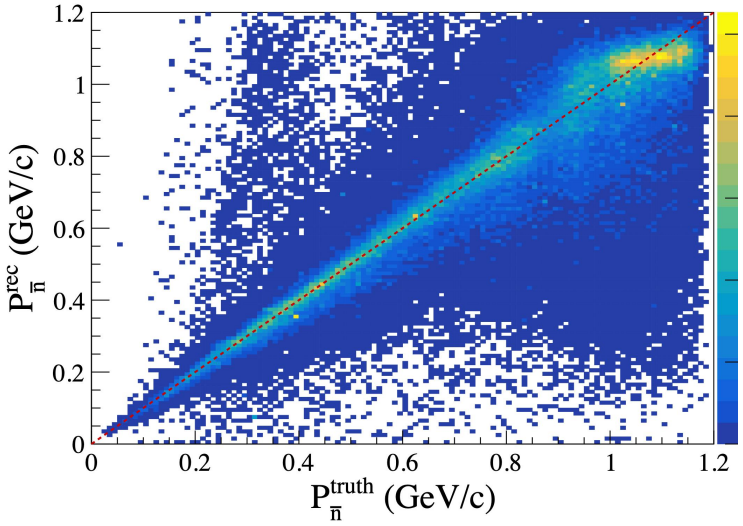
Improved TOF Reconstruction for Antineutron at BESIII:

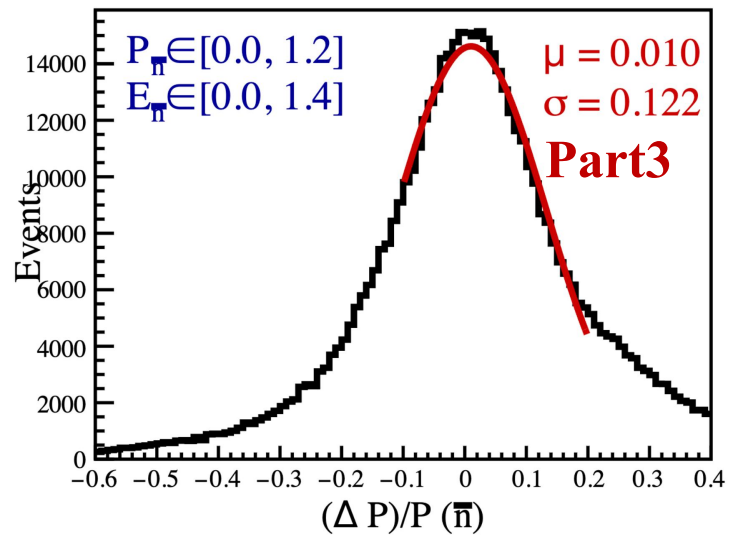
Results

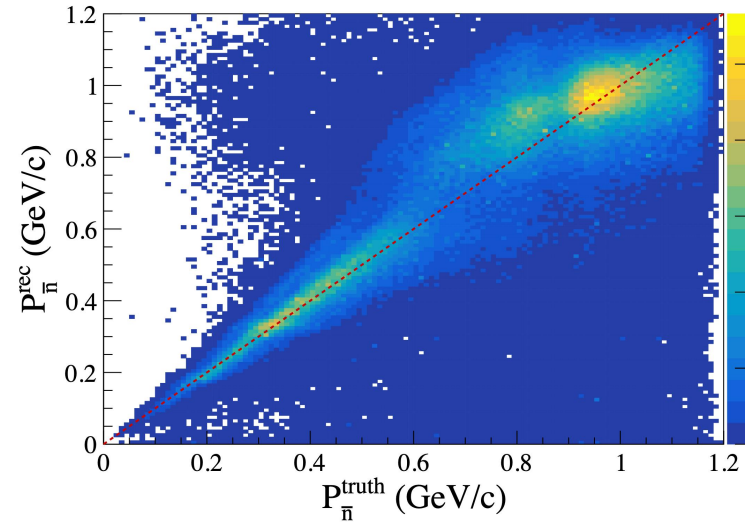






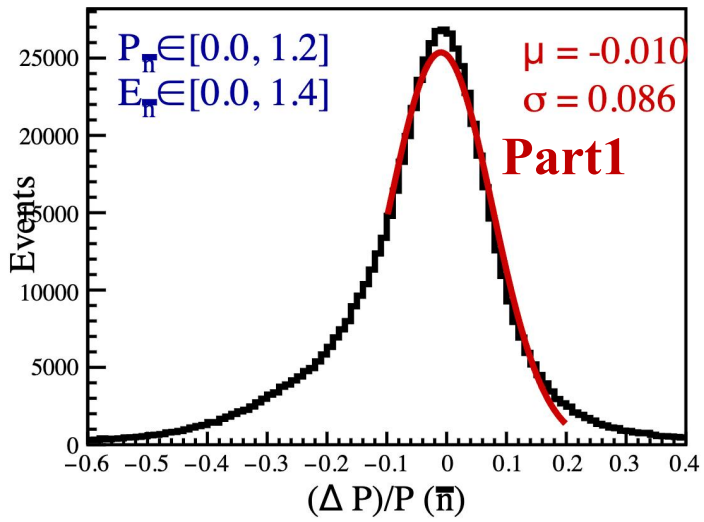


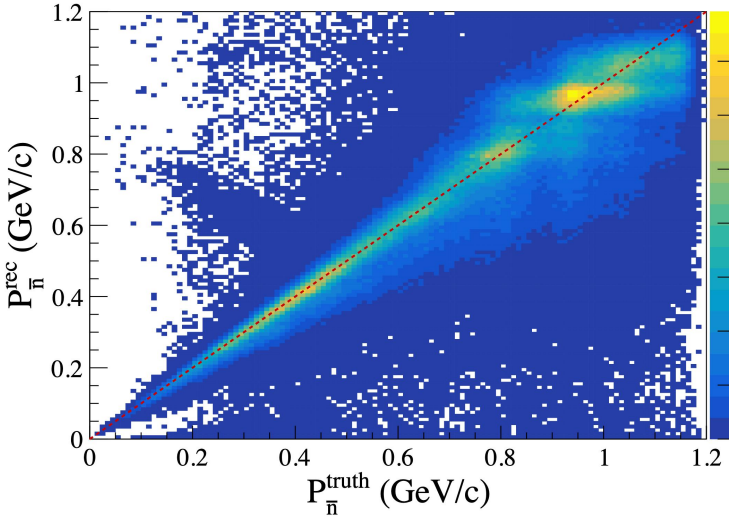


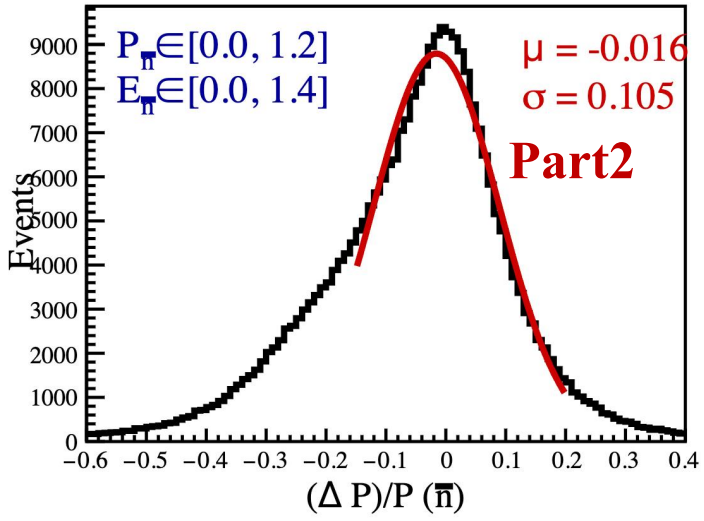


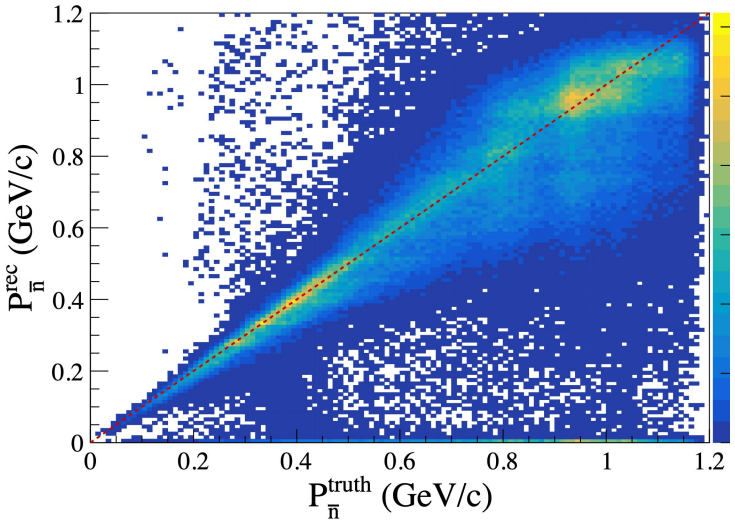
Improved TOF Reconstruction for Antineutron at BESIII:

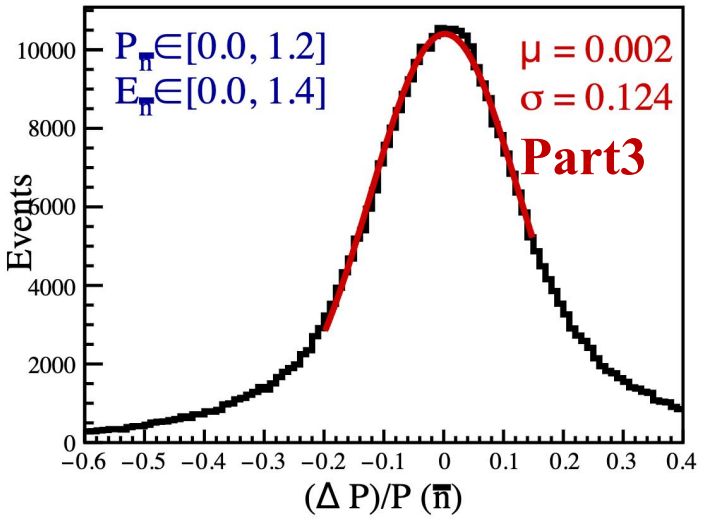
Results

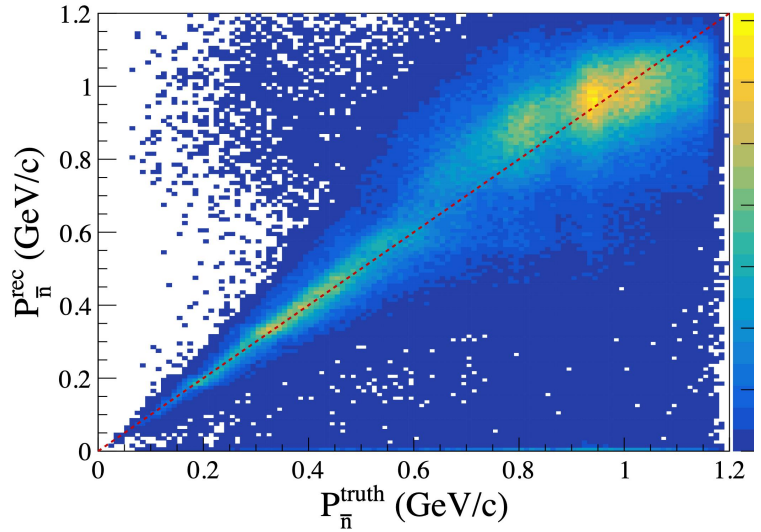






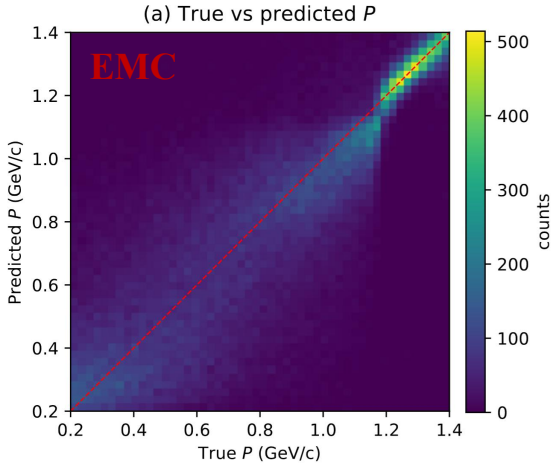


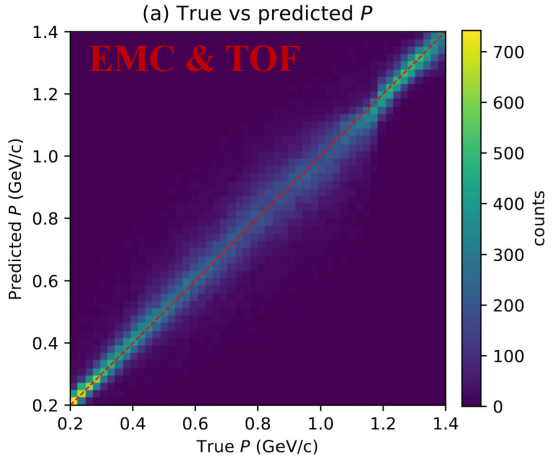


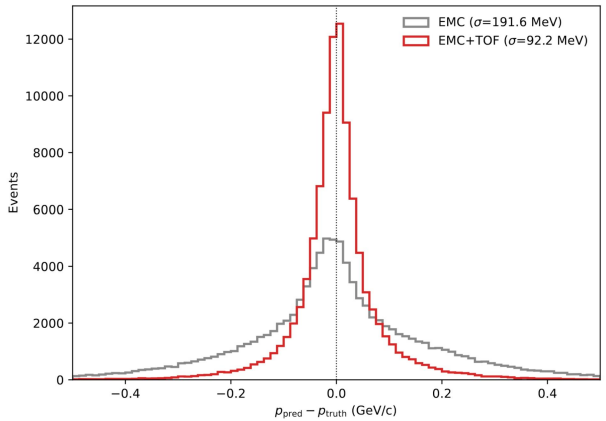


Improved TOF Reconstruction for Antineutron at BESIII:
Comparison with ML Method

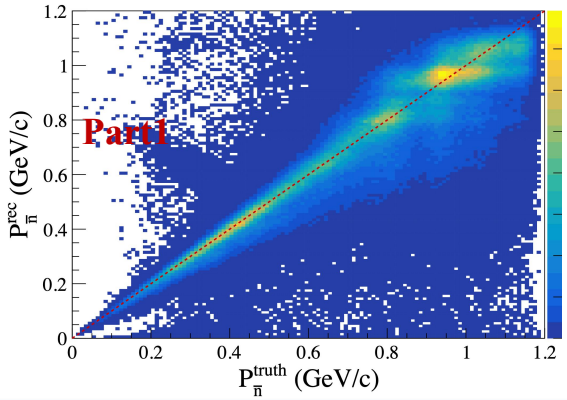
- Full reconstruction of neutral tracks by **machine learning** is going on at BESIII.
  - ✓ **MrCAL**(Mixed-representation Calorimetric Network), **EMC and TOF infos**[1].

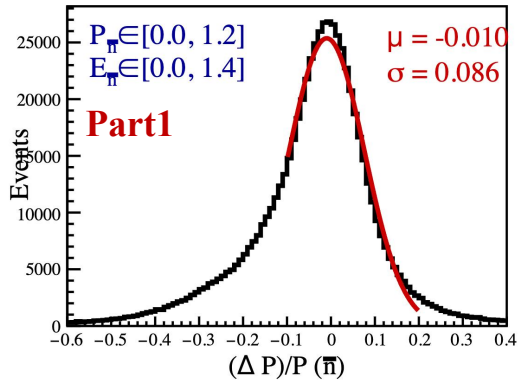






- Instead of machine learning, we adopt a **more conventional** approach.





Summary

- TOF reconstruction for $\overline{n}$ is performed.
  - ✓ The momentum resolution is **around 10%**.
  - ✓ The momentum resolution of $\overline{n}$ with low momentum is better than high momentum.
- Next to do:
  - ➢ Try to improve momentum resolution.
  - ➢ Study efficiency.
  - ➢ Try to apply to $e^+e^- \to \gamma_{\mathrm{isr}} n\overline{n}$ process.

Summary and Prospects

Summary:

- Study of $e^+e^- \to p\bar{p}$ near threshold:
  - ✓ The Born cross section has been measured with **unprecedented precision** near threshold.
  - ✓ Draft under BESIII review.
- Improved TOF reconstruction of antineutron at BESIII
  - ✓ $\bar{n}$ sample is selected to study the TOF reconstruction of antineutron.
  - ✓ The momentum resolution is **around 10%**.

Prospects:

- Continue the study of $e^+e^- \to p\bar{p}$ near threshold:
  - Angular analysis to exact $|G_E/G_M|$.
- Study of $e^+e^- \to \gamma_{\rm isr} n\bar{n}$ at 3.773 GeV.

Thank you for attention!!!

Appendix:

$\bar{p}N \rightarrow Anything$

$\bar{p}p \rightarrow Anything$

Pionic multiplicity distribution

	From Table 7	From [263]
2 pions	$0.38 \pm 0.03\%$	$0.38 \pm 0.03\%$
3 pions	$7.4 \pm 0.3\%$	$7.8 \pm 0.4\%$
4 pions	$18.1 \pm 1.8\%$	$17.5 \pm 3.0\%$
5 pions	$35.2 \pm 3.7\%$	$45.8 \pm 3.0\%$
6 pions	$23.3 \pm 2.8\%$	$22.1 \pm 1.5\%$
7 pions	$3.3 \pm 0.3\%$	$6.1 \pm 1.0\%$
8 pions		$0.3 \pm 0.1\%$

Final state	BNL		CERN
K^+K^-	1.10 ± 0.10		0.96 ± 0.08
$K_sK_s + K_lK_l$	$0.010^{+0.012}_{-0.010}$		0.008 ± 0.008
K_sK_l	0.71 ± 0.10		0.80 ± 0.05
$(K_sK_s + K_lK_l)\pi^0$	1.46 ± 0.20		1.56 ± 0.12
$K_sK_l\pi^0$	0.67 ± 0.07		0.67 ± 0.07
$(K_sK_s + K_lK_l)MM$	1.28 ± 0.16	10^{-3}	1.42 ± 0.26
$K_sK^{\pm}\pi^{\mp}$	4.25 ± 0.55		4.25 ± 0.20
$(K_sK_s + K_lK_l)\pi^-\pi^+$	4.02 ± 0.52		3.90 ± 0.46
$K_sK_l\pi^-\pi^+$	2.41 ± 0.36		2.26 ± 0.45
$K^0K^{\pm}\pi^{\mp}\pi^0$	8.94 ± 1.06		9.38 ± 1.10
$(K_sK_s + K_lK_l)\pi^-\pi^+\pi^0$	2.98 ± 0.44		2.20 ± 0.28
$K^0K^{\pm}\pi^{\mp}\pi^-\pi^+$	0.59 ± 0.08		0.71 ± 0.07
$K^0K^{\pm}4\pi$	~ 0		~ 0
Sum	28.4 ± 1.5		28.1 ± 1.4

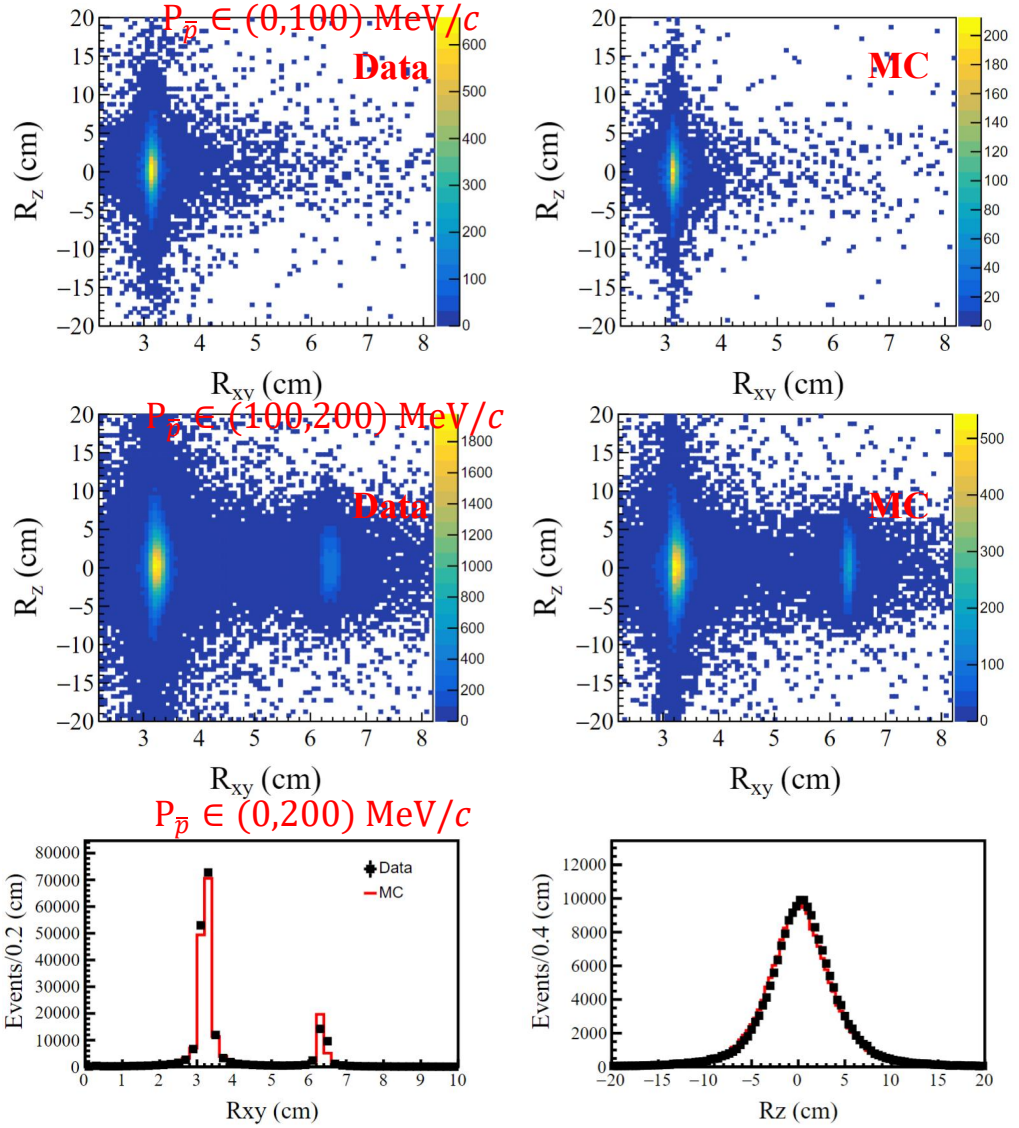
Physics Reports 413 (2005) 197 – 317

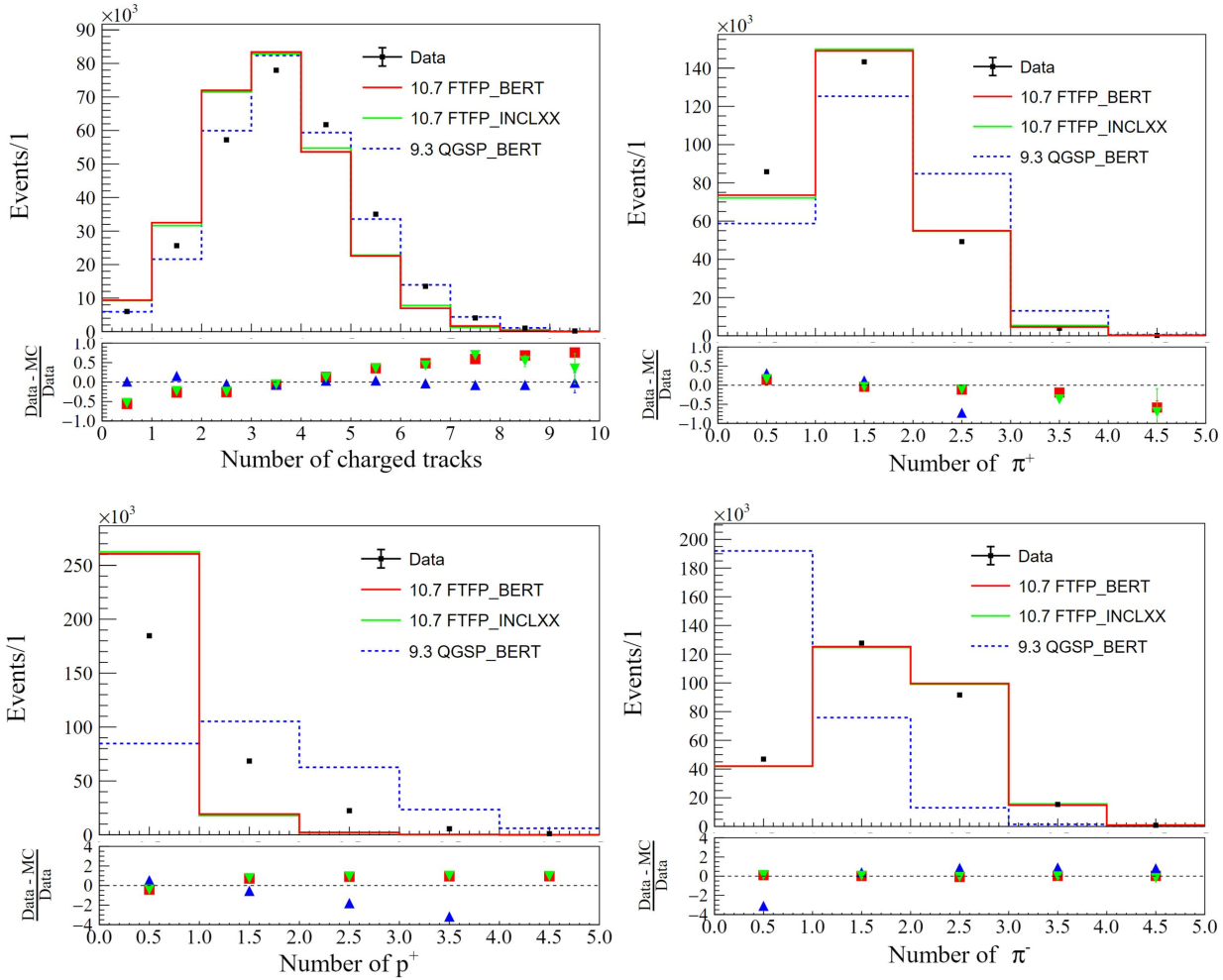
$\bar{p}n \rightarrow Anything$

Final state	Frequency (in %)
$\pi^-n\pi^0$	16.4 ± 0.5
$\pi^-\pi^0$	0.40 ± 0.04
$\pi^-2\pi^0$	0.68 ± 0.07
$\pi^-4\pi^0$	1.32 ± 0.20
$2\pi^-\pi^+n\pi^0$	59.7 ± 1.2
$2\pi^-\pi^+$	1.57 ± 0.21
$2\pi^-\pi^+\pi^0$	21.8 ± 2.2
$2\pi^-\pi^+2\pi^0$	6.3 ± 1.1
$3\pi^-2\pi^+n\pi^0$	23.4 ± 0.7
$3\pi^-2\pi^+$	5.15 ± 0.47
$3\pi^-2\pi^+\pi^0$	15.1 ± 1.0
$4\pi^-3\pi^+n\pi^0$	0.39 ± 0.07
Sum	$95.5 \pm 1.5\%$

Final state	Frequency (in 10^{-4})
K^0K^-	14.7 ± 2.1
$K^0K^+\pi^-\pi^-$	36.0 ± 4.2
$K_sK_s\pi^-$	14.7 ± 2.0
$K_sK_l\pi^-$	21.2 ± 3.6
$K^0K^+\pi^-\pi^-$	24.8 ± 2.6
$K^0K^-\pi^+\pi^-$	34.2 ± 3.5
$K_sK_s\pi^-\pi^0$	25.6 ± 2.8
$K^0K^+\pi^-\pi^-\pi^0$	1.6 ± 0.9
$K_sK^-\pi^+\pi^-\pi^0$	33.6 ± 3.8
$K_sK^-\omega$	35.0 ± 5.2
$K_sK_s\pi^+\pi^-\pi^-$	2.8 ± 1.2
$K_sK_l\pi^+\pi^-\pi^-$	1.9 ± 1.2
Sum	$2.5 \pm 0.1\%$

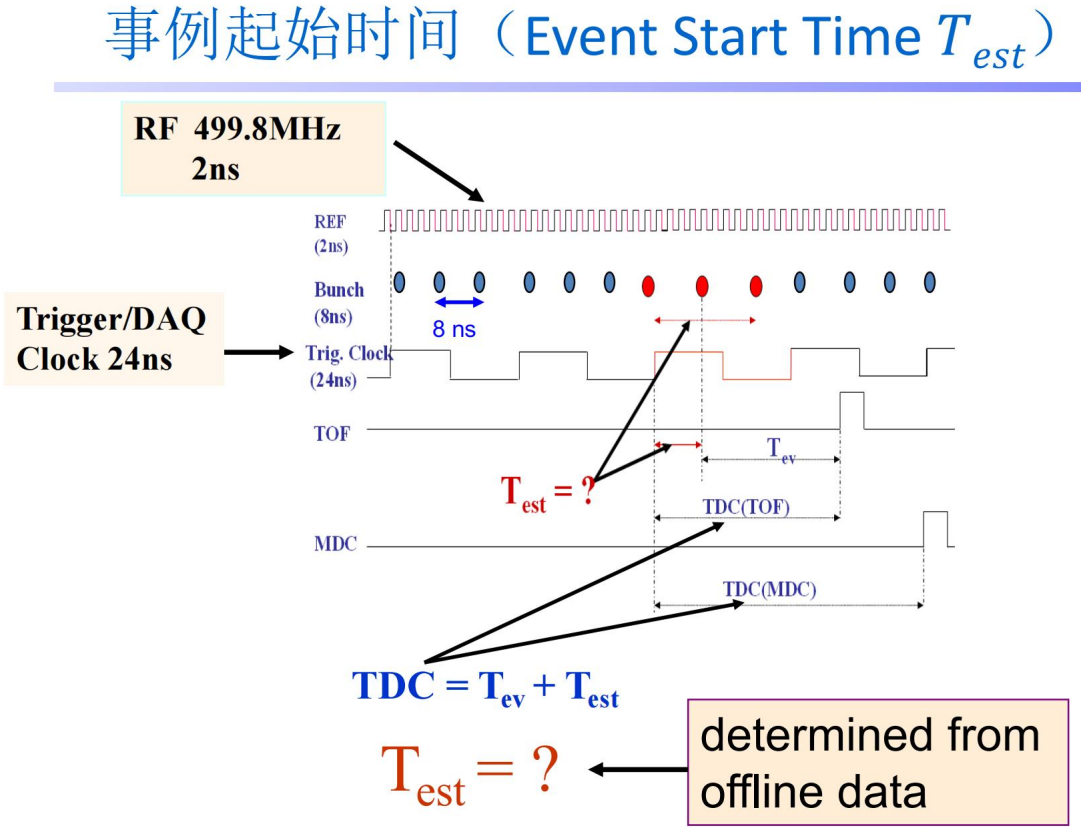
Appendix:
Control sample





Appendix:
T0 mismatch

- The determination of the event start time is the first step in event reconstruction at BESIII.



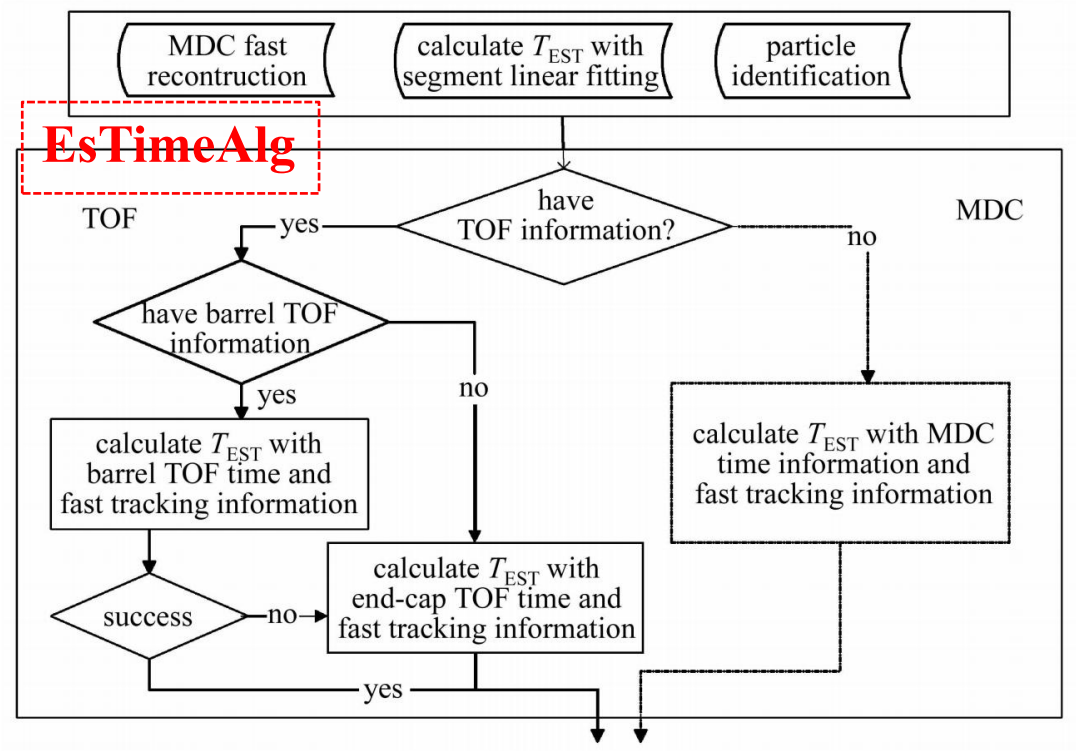
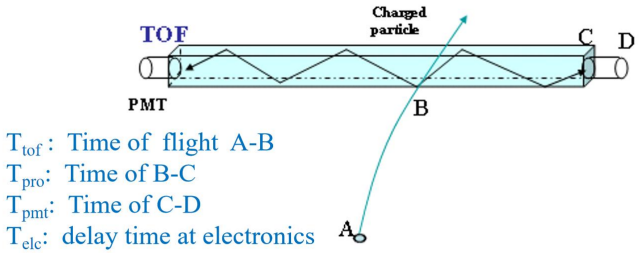


Fig. 2. The event start time programme flow.

✓ MDC Fast Tracking, dE/dx, EMC, PID...

Appendix:
T0 mismatch: Case I

Use TOF to calculate T_{est}



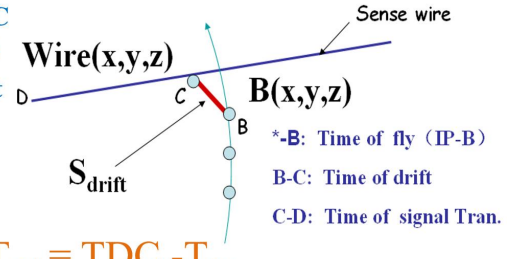
T_{tof} : Time of flight A-B
T_{pro}: Time of B-C
T_{pmt}: Time of C-D
T_{elc}: delay time at electronics

$T_{est} = TDC - T_{ev}$

$T_{ev} = T_{tof} + T_{pro} + T_{pmt} + T_{elc}$

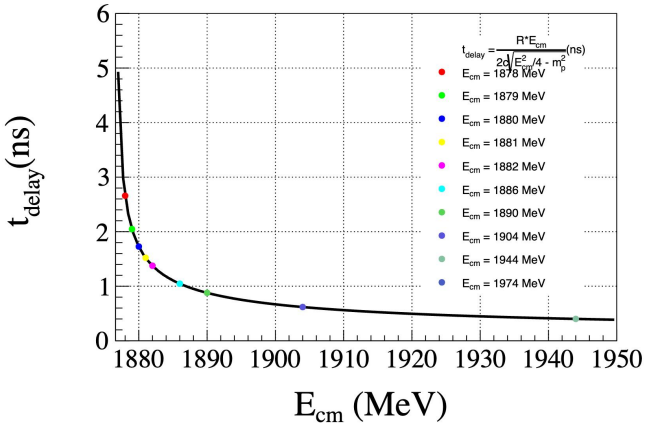
Use MDC to calculate T_{est}

T_f : Time of flight A-B
T_{drift}: Time of B-C
T_{wp}: Time of C-D
T_{elc}: delay time at electronics



$T_{est} = TDC - T_{ev}$

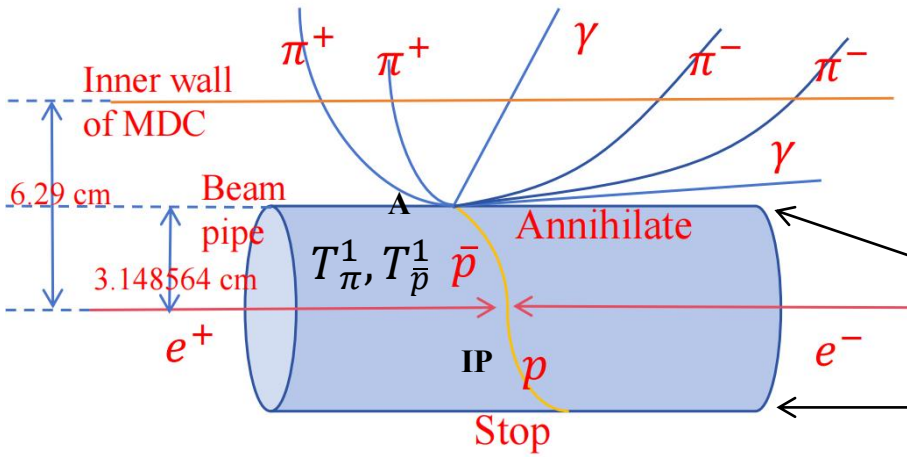
$T_{ev} = T_f + T_{drift} + T_{wp} + T_{elc}$

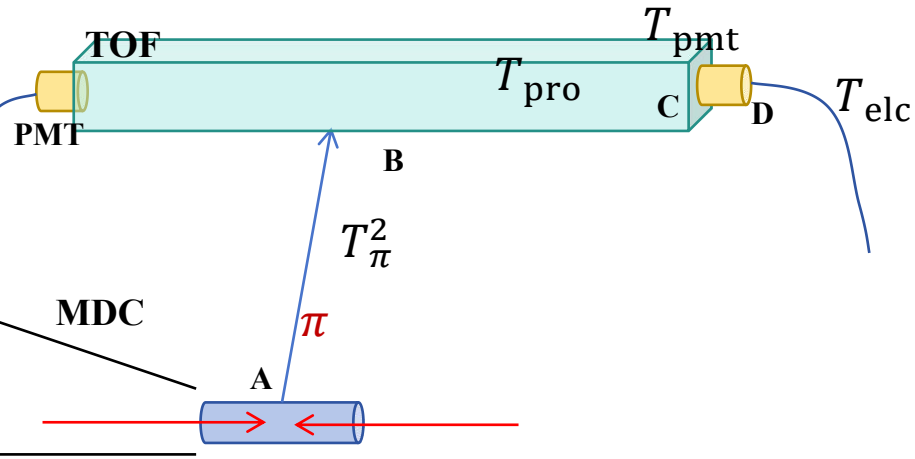


True case: $T_{tof} = T_{\bar{p}}^1$(before annihilation) $+ T_{\pi}^2$

But in Alg: $T_{tof} = T_{\pi}^1$~~(before annihilation)~~ $+ T_{\pi}^2$

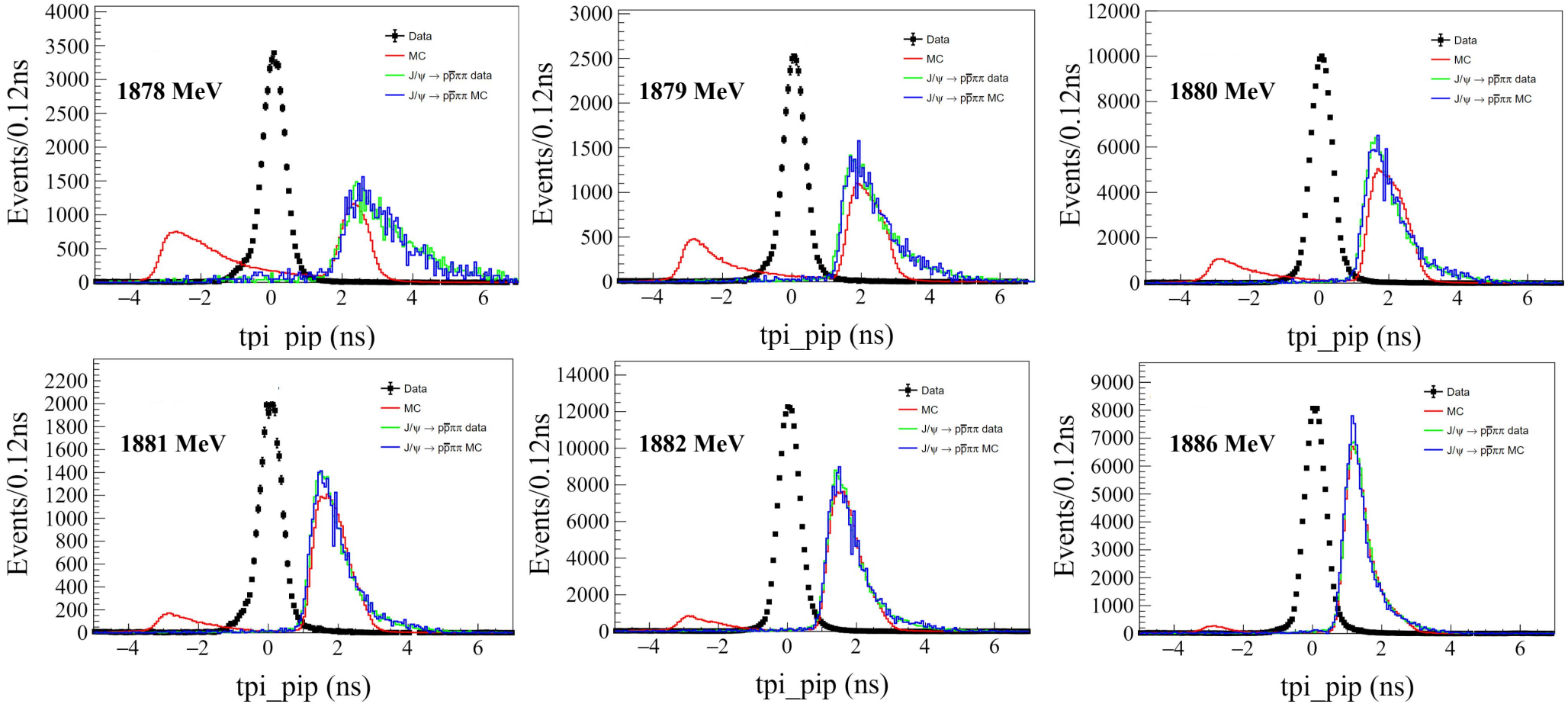
T_{ev} is underestimated, T_{est} is overestimated.
If $T_{\bar{p}}$ large than 3ns, T_0 will mismatch.



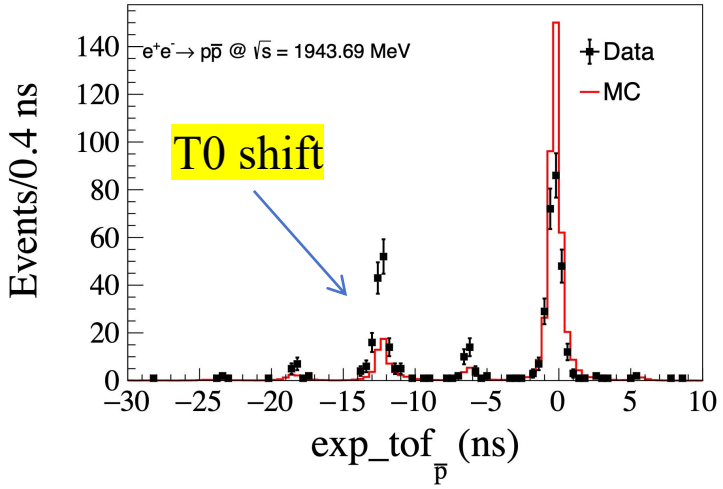


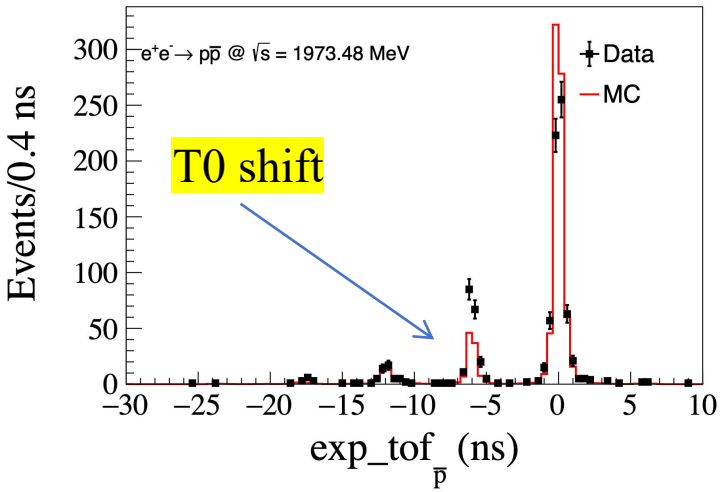
Appendix:
T0 mismatch: Case I

- $t_{\pi^{\pm}}$: $Tof_{\pi^{\pm}} - T^{exp}_{\pi^{\pm}}$

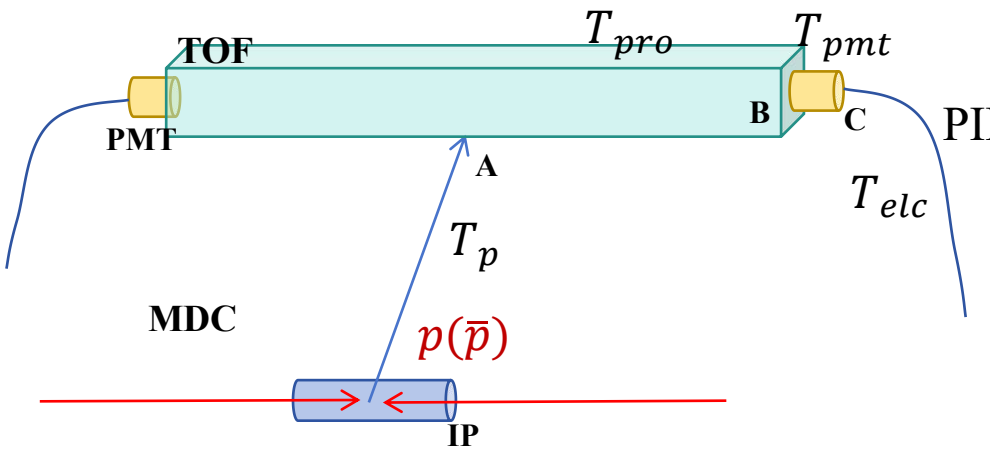


Appendix:
T0 mismatch: Case II



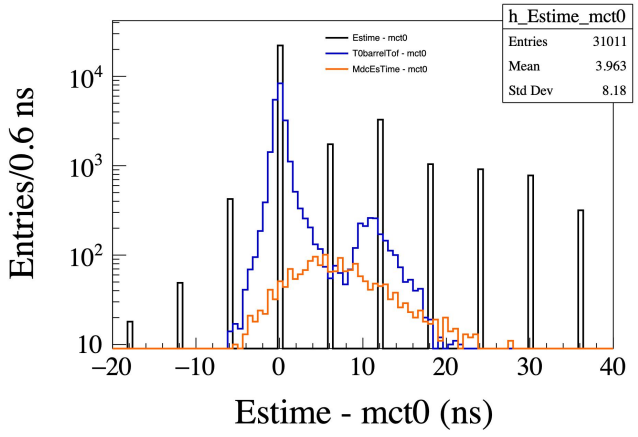


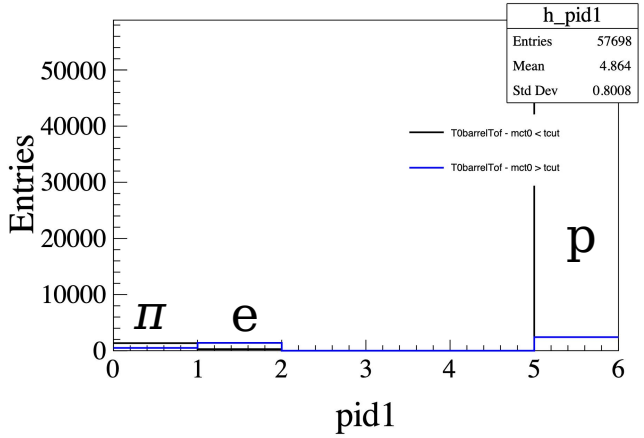
$$T_{ev} = T_{tof} + T_{pro} + T_{pmt} + T_{elc}\,; \quad T_{tof} = T_p$$



PID for $e/p/\pi$:

- ✓ use E/p to identify $e^{\pm}$.
- ✓ use dE/dx to identify $p(\bar{p})$.
- ✓ others are regarded as $\pi^{\pm}$.

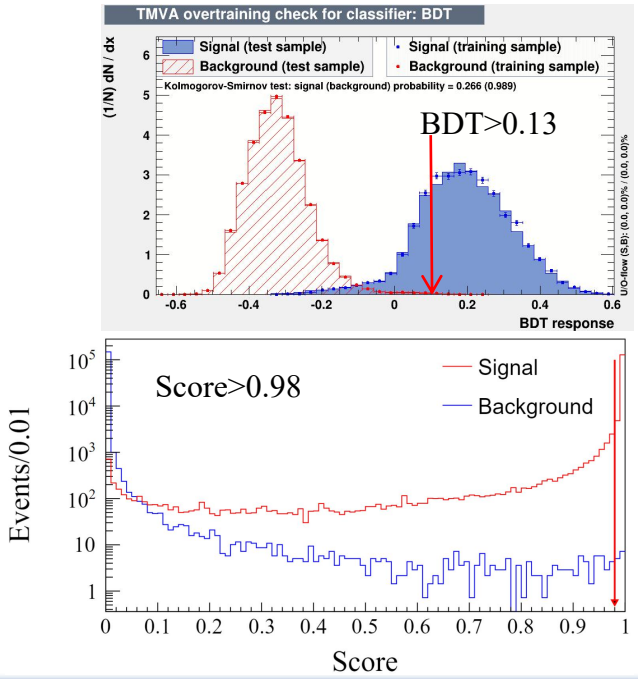


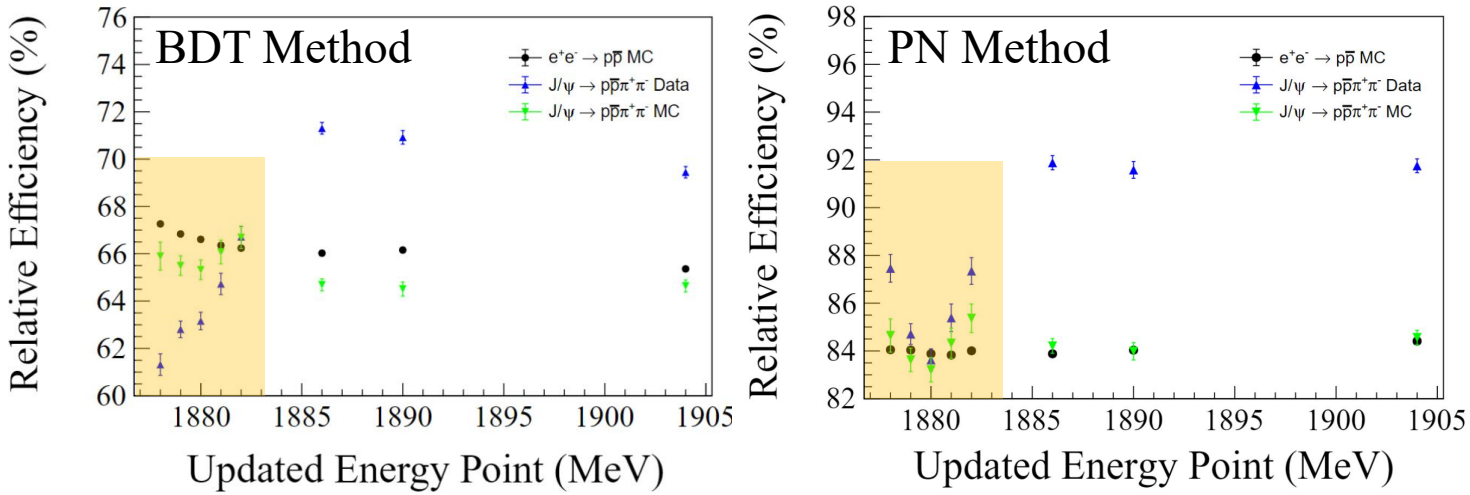


$$t_e = \frac{81cm}{30\,cm/ns} \cong 2.7ns \qquad t_p = \frac{81cm}{0.2 * 30\,cm/ns} \cong 13.5ns$$

Appendix:
Machine Learning Method

- Some ML methods are used to supress the backgrounds: MVA(BDT), GNN(Particle Net).
  - ➢ Training was conducted using data below the threshold (as background, @1.840, 1.870 GeV) and control sample data (as signal, with $P_{\bar{p}} < 0.1$ GeV), and the trained model was applied to all energy point data and MC.
  - ➢ Simply using the 1.870 GeV data and nnbar MC to estimate background events.
- Compare the ML relative efficiency given by $p\bar{p}$ MC and $J/\psi \to p\bar{p}\pi^+\pi^-$ control sample:





✓ Take GNN method as the nominal one, and BDT as a cross-check.

Appendix:
Machine Learning Method

Features of Changed Tracks:

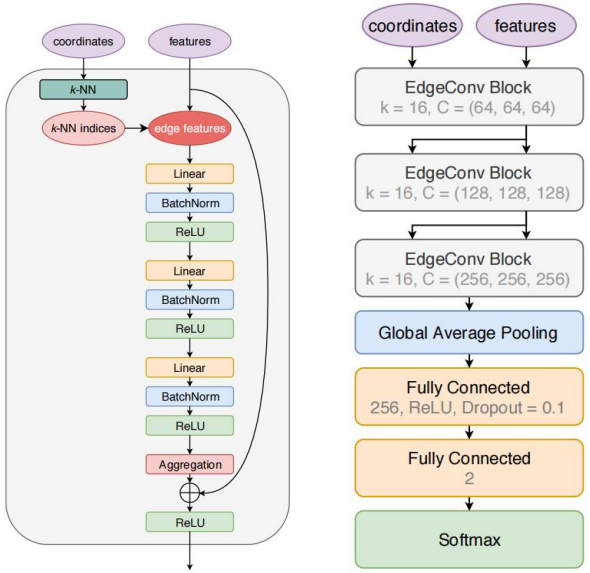
- **Azimuth angle:** ϕ and θ in lab frame.
- **Charge:** the charge of track.
- **Momentum:** the momentum of track. To achieve better resolution, this feature is obtained from `RecMdcKalTrack` after Kalman filter.
- **Helix parameters:** the five helix parameters $(d_\rho,\ d_z,\ \kappa,\ \phi_0,\ \lambda)$ describing the spatial trajectory of track.
- $\chi_{\mathrm{d}E/\mathrm{d}x}$**:** the four variables describing the divergence of $\mathrm{d}E/\mathrm{d}x$ measurement from its expected values under electron, pion, kaon and proton hypotheses, respectively.

Points of Tracks:

- (θ, ϕ) as the position of particles.

$$\boldsymbol{x}_i' = \square_{j=1}^{k} \boldsymbol{h}_{\boldsymbol{\Theta}}(\boldsymbol{x}_i, \boldsymbol{x}_{i_j}),$$

$$\boldsymbol{h}_{\boldsymbol{\Theta}}(\boldsymbol{x}_i, \boldsymbol{x}_{i_j}) = \bar{\boldsymbol{h}}_{\boldsymbol{\Theta}}(\boldsymbol{x}_i, \boldsymbol{x}_{i_j} - \boldsymbol{x}_i),$$



Features of Neutral Tracks:

- **Azimuth angle:** ϕ and θ in lab frame.
- **Energy:** the energy of this shower.
- **Hit Number:** the number of hitting crystals in EMC.
- **Time:** the time information of shower.
- E_{III} **and** E_V**:** the ratio of energy deposited in the 3×3 or 5×5 crystal around the center of the shower, respectively.
- A_{20} **moment and** A_{42} **moment:** the Zernike moment A_{nm} defined as

$$A_{n,m} = \left| \sum_i \frac{E_i}{E_{tot}} f_{n,m}(r_i/R_0) e^{im\phi} \right|, \tag{9}$$

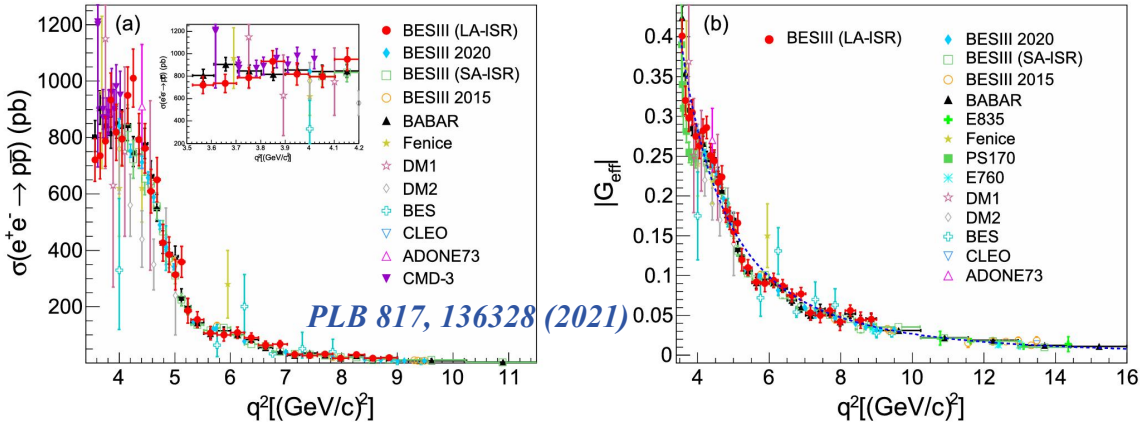
with $f_{2,0}(x) = 2x^2 - 1$ and $f_{4,2} = 4x^4 - 3x^2$. Here i denotes the different crystals, E_i is the energy deposited in the crystal and r_i is its distance from the shower center.

- **Secondary moment:** defined as $\sum_i E_i r_i^2 / \sum_i E_i$.
- **lateral moment:** defined as $\sum_{i=3}^{n} E_i r_i^2 / (E_1 r_0^2 + E_2 r_0^2 + \sum_{i=3}^{n} E_i r_i^2)$.

Study of $e^+e^- \to p\bar{p}$ near threshold:

Motivation

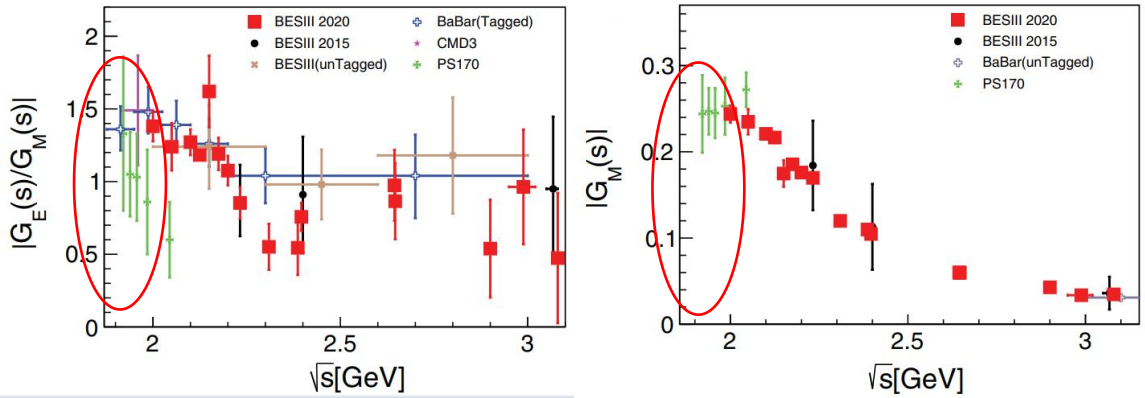
- The Born cross section for $e^+e^- \to p\bar{p}$ has been measured by many experiments:
  - ✓ Both **scan and ISR** method.
  - ✓ Energy dependent lineshape.
  - ✓ **Fewer** measurements with **large** uncertainty near threshold.



PLB 817, 136328 (2021)

- Various theoretical models describe time-like form factors in non-perturbative region:
  - ✓ ChEFT, VMD, Relativistic CQM, parton model, pQCD etc.
  - ✓ Experimental data near the threshold are **very scarce**.

PRL 124, 042001(2020)



Improved TOF Reconstruction for Antineutron at BESIII:
$n/\bar{n}$ Sample

- Anti-proton control sample is selected from $J/\psi \to p\bar{n}\pi^- + cc.$ data, and here is the event selection:

  - **Good Charged Track:**

    $|\cos\theta| \leq 0.93$; $|V_{xy}| < 0.5$ cm; $|V_z| < 5.0$ cm; $N_{charged} \geq 2$;

  - **PID:** use dE/dx and TOF information

    p: prob(p)>prob(π, K)

    π: prob(π)>prob(p, K)

    K: prob(K)>prob(π, p)

    $N_p \geq 1$ and $N_\pi \geq 1$

  - **Vertex fit:**

    Loop all the $p\pi$ tracks, and select the combination with minimum χ^2_{VF}

  - **Kinematic fit:**

    Missing 3-momentu of $\bar{n}/n$, do 1C kinematic fit, χ^2_{KF}

  - **Recoil $\bar{n}$:**

    $P_{\bar{n}/n} = P_{cms} - P_p - P_\pi$ with 4-mom before Kinematic fit.

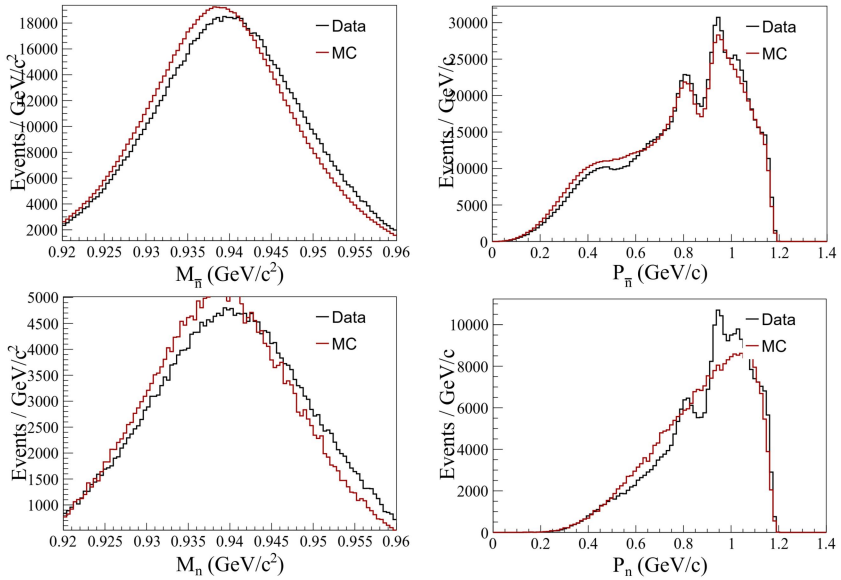
  - **Further Selection:**

    $0.92 < M_{\bar{n}/n} < 0.96$ GeV/c^2, $\chi^2_{VF} < 20$, $\chi^2_{KF} < 10$,

  - **Select $\bar{n}/n$:**

    Select good photon, and take the leading shower as $\bar{n}/n$ candidate.

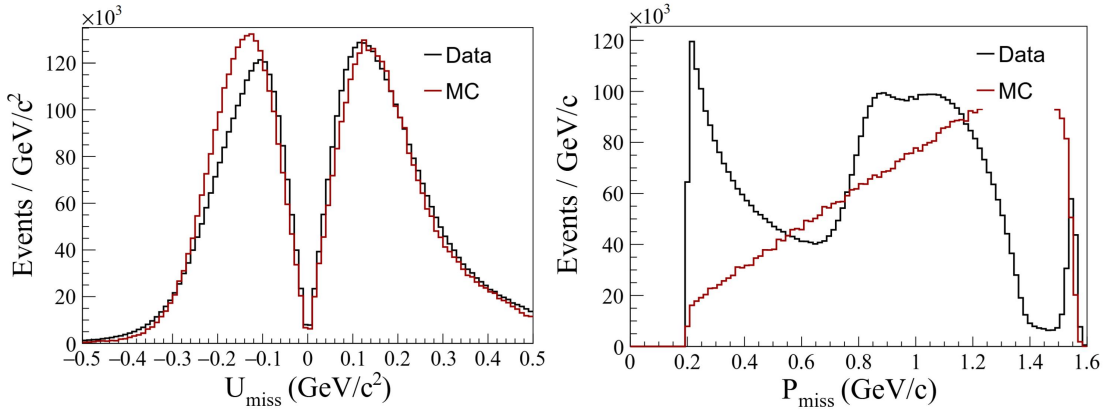
    $\mathrm{dAng}_{\gamma\bar{n}/n} < 15/10°$



Improved TOF Reconstruction for Antineutron at BESIII:

γ Sample

- Gamma control sample is selected from $J/\psi \to \gamma e^+ e^-$ data, and here is the event selection:
  - **Good Charged Track:**
    $|\cos\theta| \leq 0.93$; $|V_{xy}| < 0.5$ cm; $|V_z| < 5.0$ cm; $N_{charged} = 2$; $Q_{net} = 0$;
  - **PID:** use dE/dx and TOF information
    e: prob(e)>prob(π, K, p), prob(e)>0.0001
    , E/p>0.8
    $N_{e^+} = 1$ and $N_{e^-} = 1$
  - **Select γ:**
    Select good photon, $N_\gamma \geq 1$
  - **Vertex fit:**
    Vertex fit for the ee tracks.
  - **4C Kinematic fit:**
    Loop all the good photon, do 4C kinematic fit, select the the photon with smallest χ^2_{KF}, and require $\chi^2_{KF} < 200$.
  - **Further Selection:**
    $-0.5 < U_{miss} < 0.5$ GeV/c^2, $P_{miss} > 0.2$ GeV/c



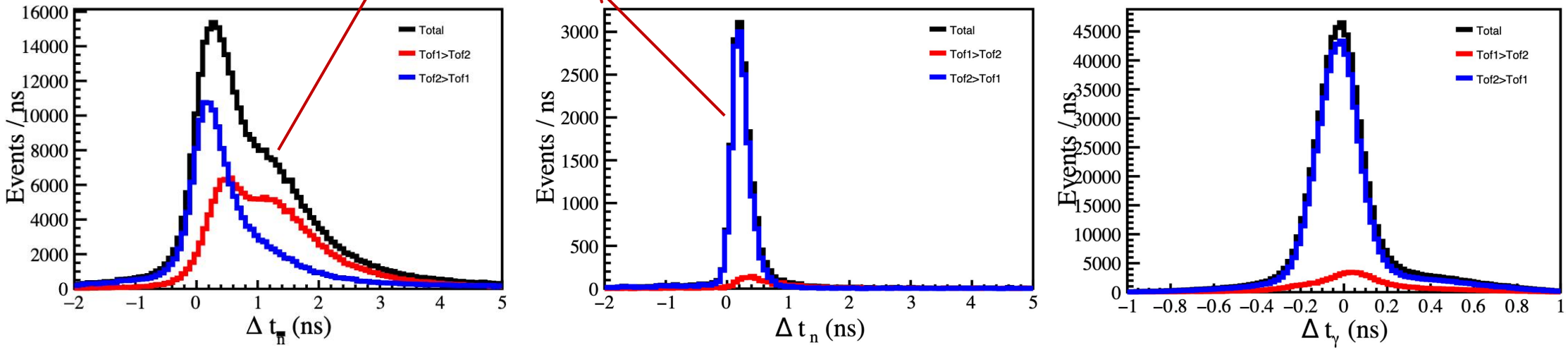
Improved TOF Reconstruction for Antineutron at BESIII:
$n/\bar{n}/\gamma$ Sample

- $n/\bar{n}/\gamma$ control samples are used to study the TOF reconstruction of neutral tracks.
  - ✓ $n/\bar{n}$ sample is selected from $J/\psi \to p\bar{n}\pi^- + cc.$ data.
  - ✓ γ sample is selected from $J/\psi \to \gamma e^+ e^-$ data.

- The TOF reconstruction gives $t_{\rm mea}$ and $t_{\rm exp(\gamma)}$.
  - ✓ $\Delta t_{\bar{n}/n/\gamma} = \boldsymbol{t_{\rm mea} - t_0 - t_{\rm exp(\bar{n}/n/\gamma)}}$

- $t_{\rm mea}$ is the matched tof hit time.
- t_0 is the event start time.
- $t_{\rm exp(\bar{n}/n)} = t_{\rm exp(\gamma)}/\beta_{\bar{n}/n}$.
- $t_{\rm exp(\gamma)} = L_{\rm exp}/c$.

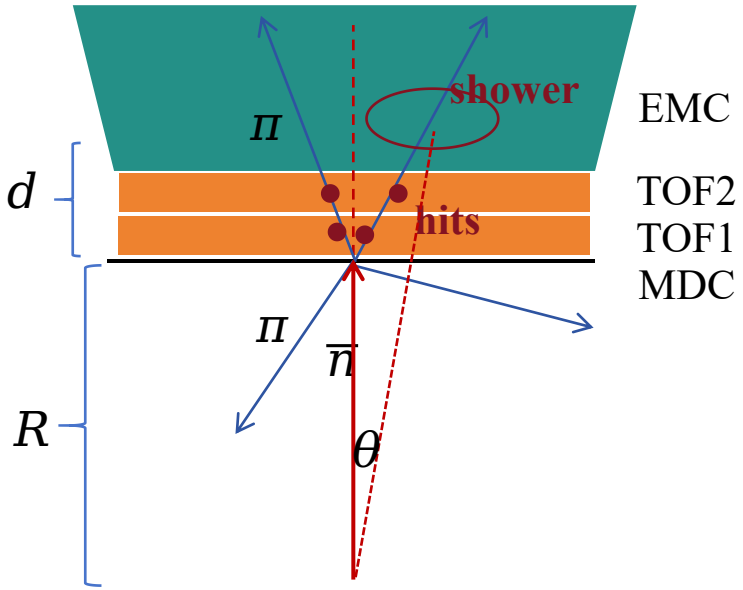
Some strange shifts → **How to understand?** → **Perform calibration**

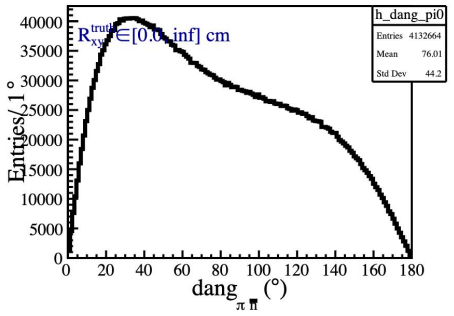


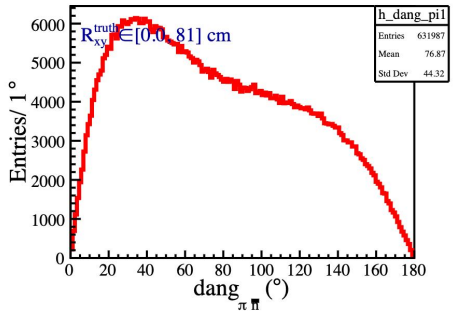
Information from Geant4

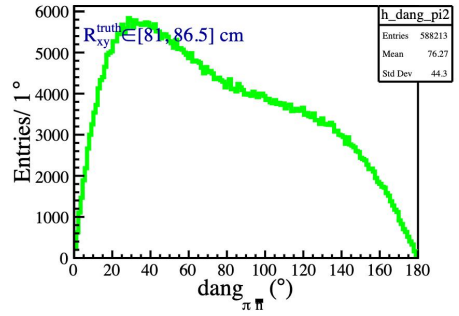
- Process Name: anti_neutronInelastic
- Typical process:
  - ✓ $R_{xy} = 3.2$ cm: $\overline{n} + Be(9) \rightarrow \pi^+ + \pi^0 + K^- + K_s + 2\alpha$
  - ✓ $R_{xy} = 80$ cm: $\overline{n} + C(12) \rightarrow B(10) + 2\pi^+ + 2\pi^- + p$
  - ✓ $R_{xy} = 84$ cm: $\overline{n} + p \rightarrow 2\pi^+ + \pi^- + 3\pi^0$
  - ✓ $R_{xy} = 87$ cm: $\overline{n} + p \rightarrow \pi^+ + 3\pi^0$
  - ✓ $R_{xy} = 87$ cm: $\overline{n} + C(12) \rightarrow \pi^+ + 4\pi^0 + p + 2n + 2\alpha$
  - ✓ $R_{xy} = 90$ cm: $\overline{n} + C(12) \rightarrow 2\pi^+ + 2\pi^- + p + D + 2\alpha$
  - ✓ $R_{xy} = 103$ cm: $\overline{n} + Cs(133) \rightarrow Sn(116) + \pi^+ + 3\pi^0 + \pi^- + 10n + 4p + D + \eta + 2\gamma$
  - ✓ $R_{xy} = 118$ cm: $\overline{n} + I(127) \rightarrow Sn(117) + 2\pi^+ + \pi^- + 2\pi^0 + 7n + 2p + 2\gamma$
  - ✓ $R_{xy} = 127$ cm: $\overline{n} + Fe(56) \rightarrow Mn(53) + 3\pi^+ + 2\pi^- + 2n + 3\gamma$
  - ✓ $R_{xy} = 150$ cm: $\overline{n} + Al(27) \rightarrow Ne(21) + n + \overline{n} + p + \alpha + 2\gamma$

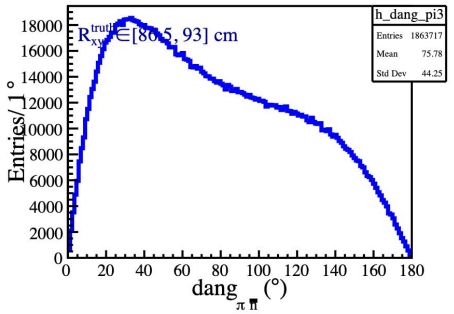
Different Parts

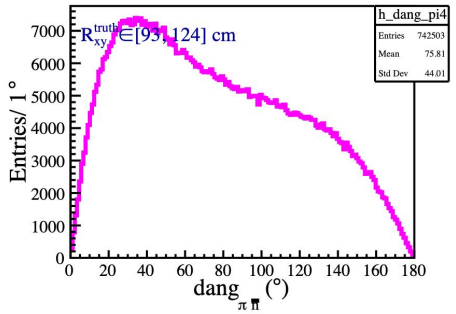


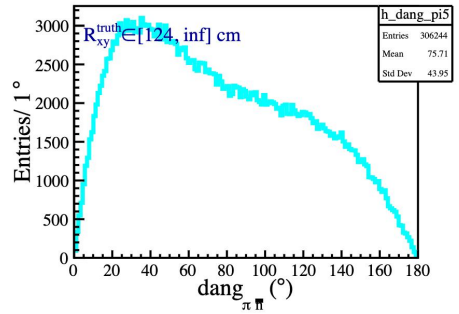










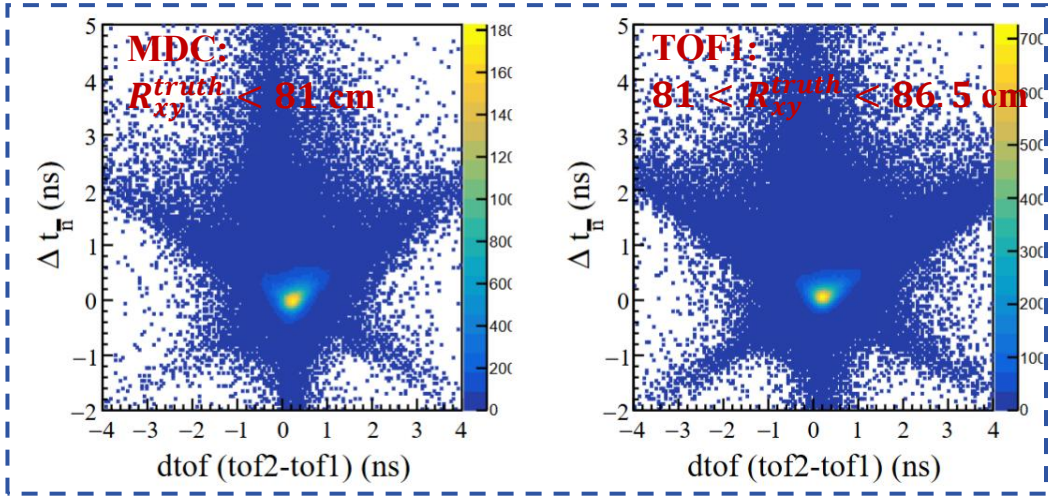


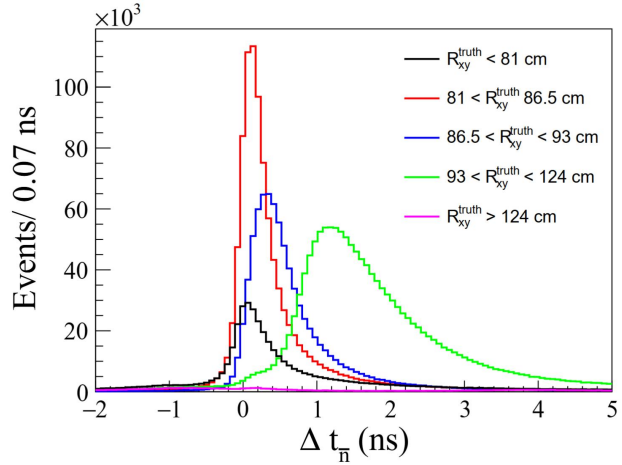
$$\theta = arctan(\frac{d * tan(dang_{\pi\bar{n}})}{d + R})$$

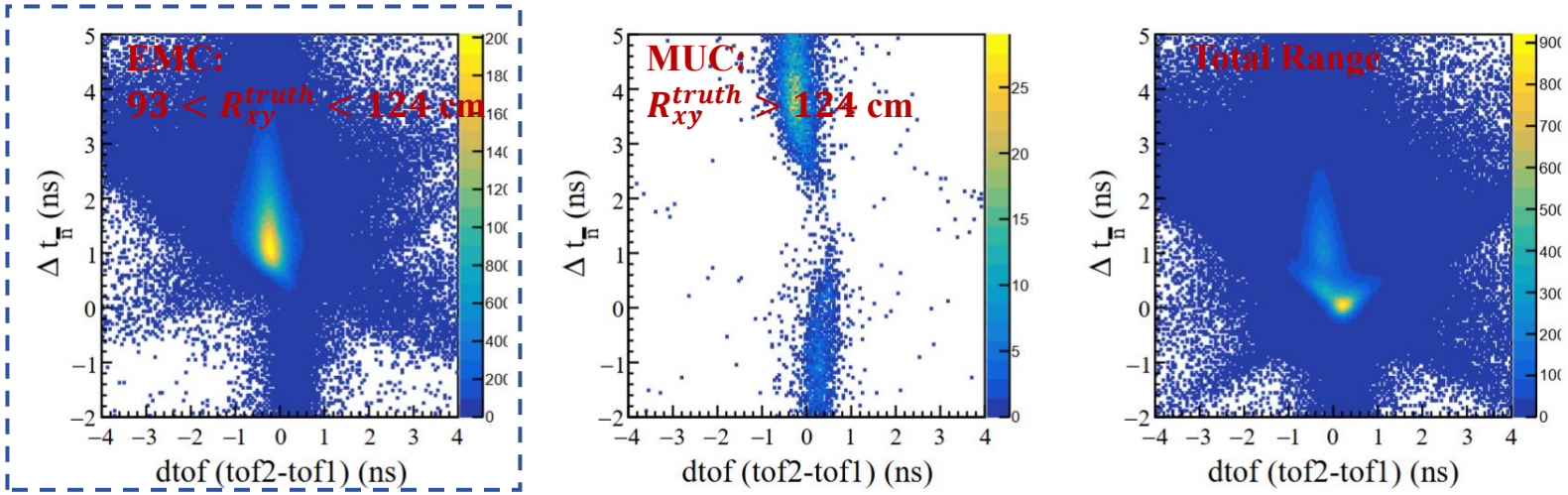
$$\theta = arctan(\frac{15 * tan(30°)}{15 + 81}) \approx 5°$$

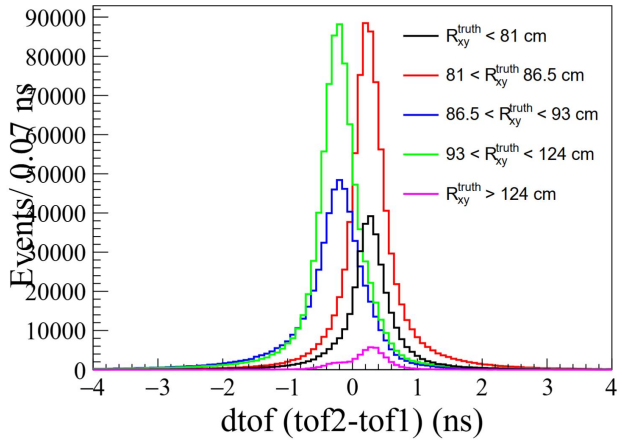
Improved TOF Reconstruction for Antineutron at BESIII:
Study $\Delta t_{\bar{n}}$

- Study $\Delta t_{\bar{n}}$ **by MC**, related to R_{xy}^{truth} and dtof (tof2-tof1).



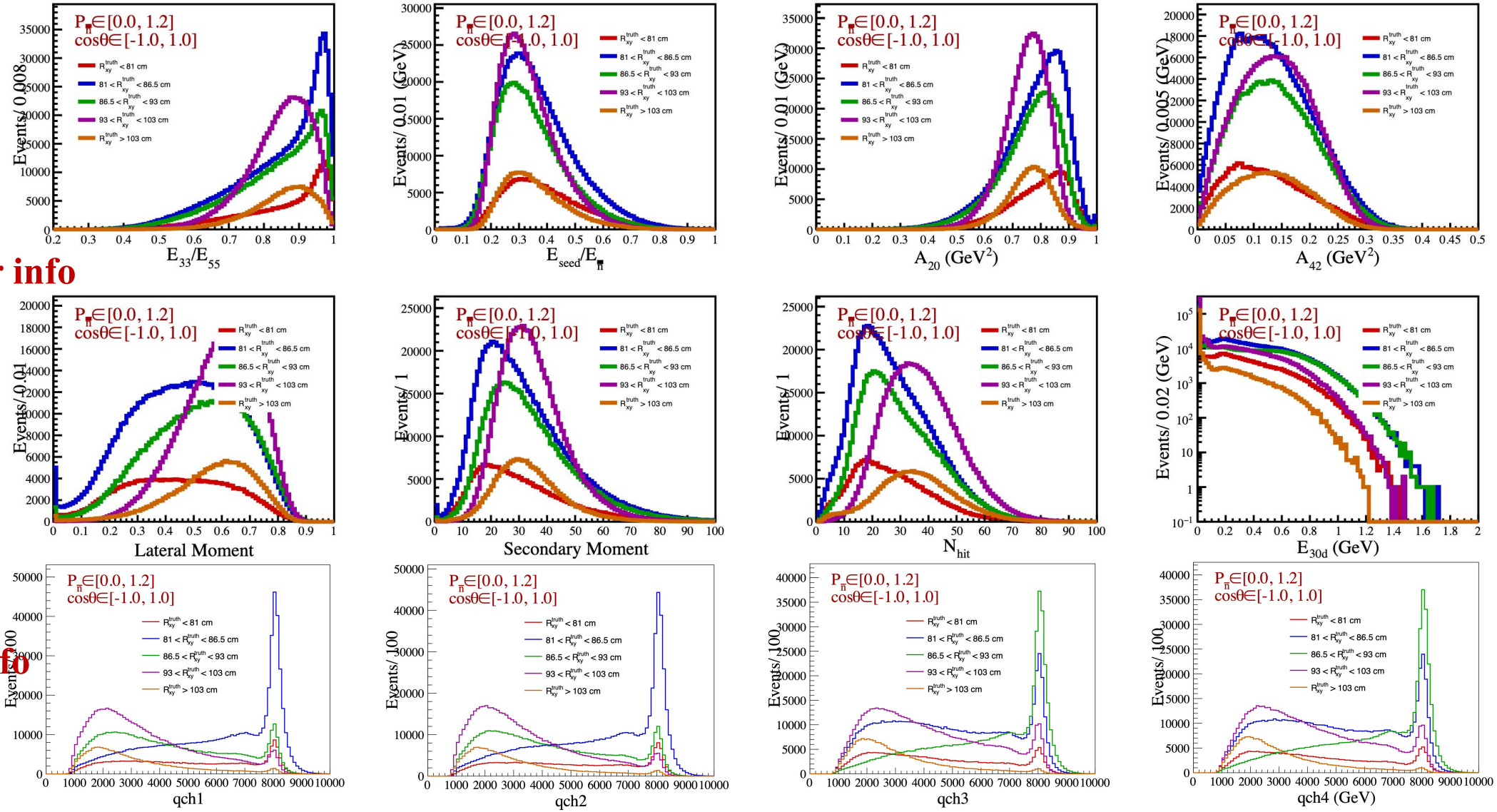






Improved TOF Reconstruction for Antineutron at BESIII:
Comparison

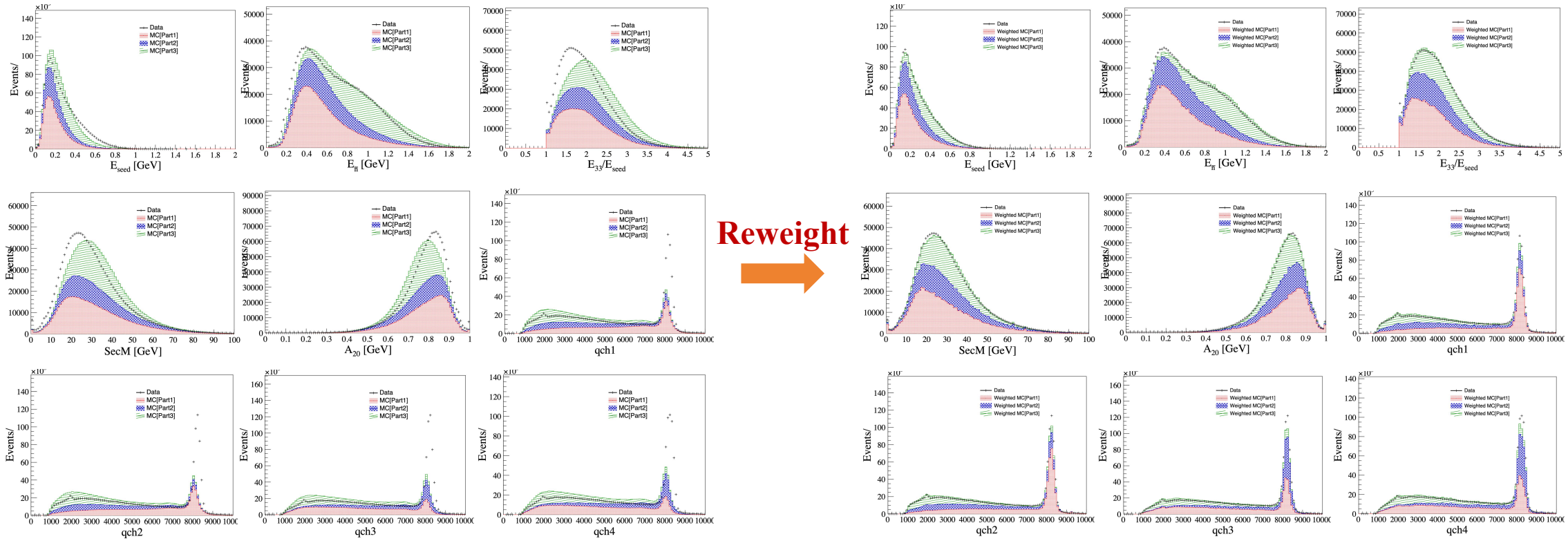
- ✓ **Shower info**
- ✓ **TOF info**



Improved TOF Reconstruction for Antineutron at BESIII:

MC Reweight

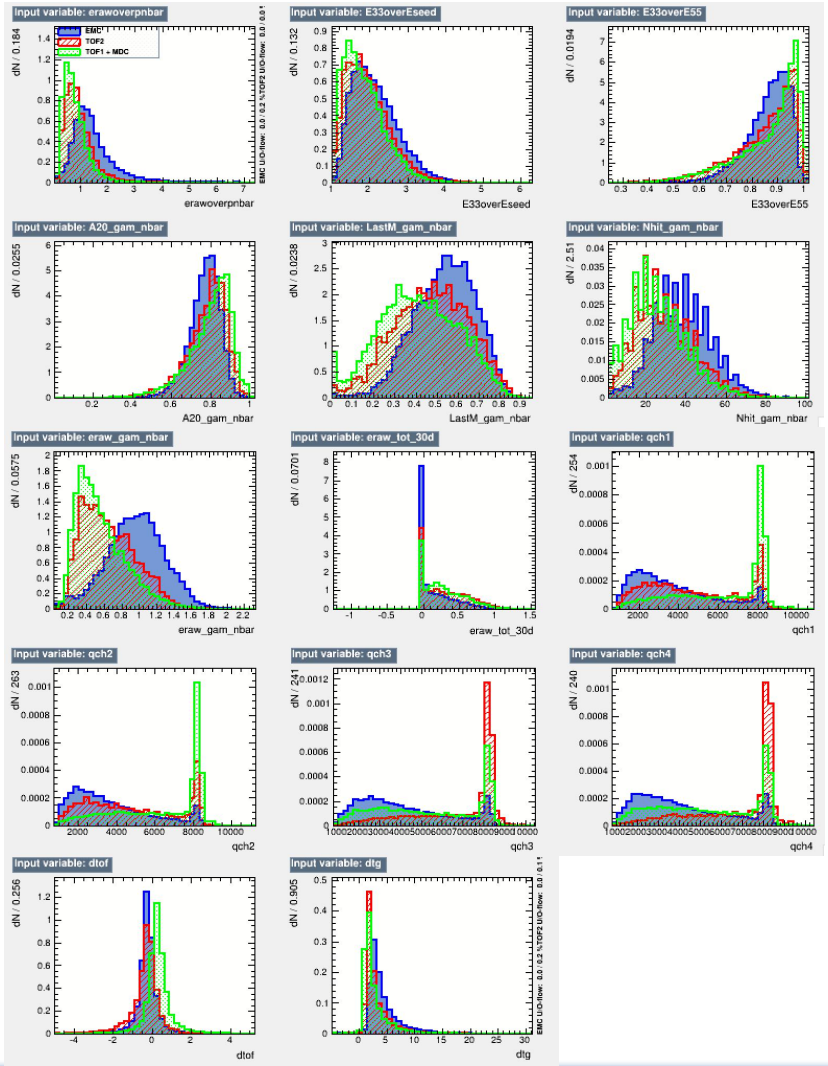
- A machine learning method(XGBoost) was used to reweight MC to data, and the variables Eseed, Nhit, Enbar, qch1234 are used.

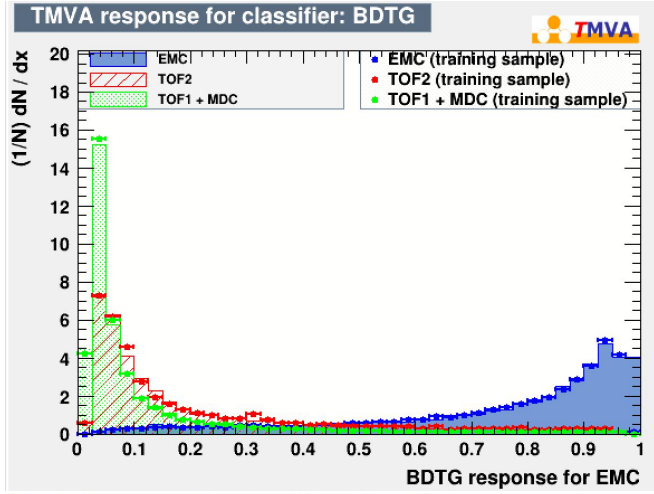


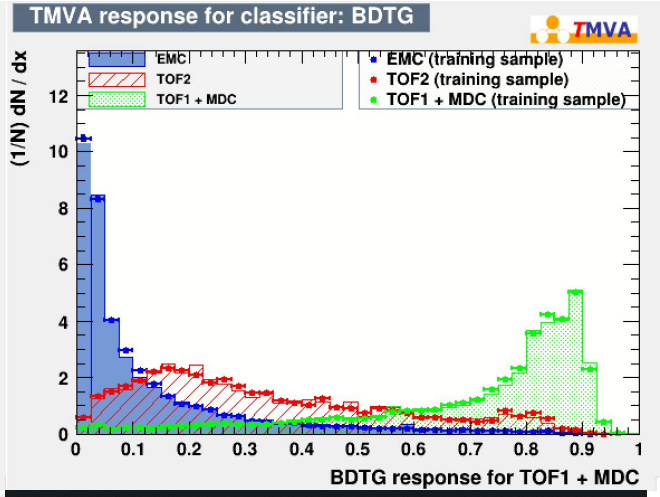
TOF Reconstruction for Antineutron at BESIII:

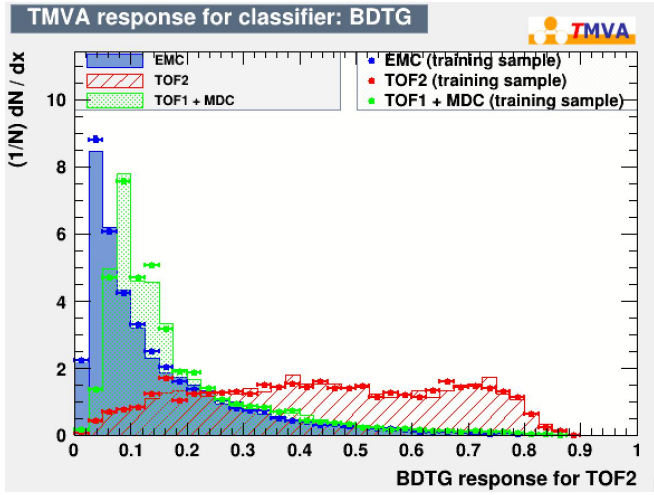
BDTG Training

- Training a BDTG to distinguish these three parts.









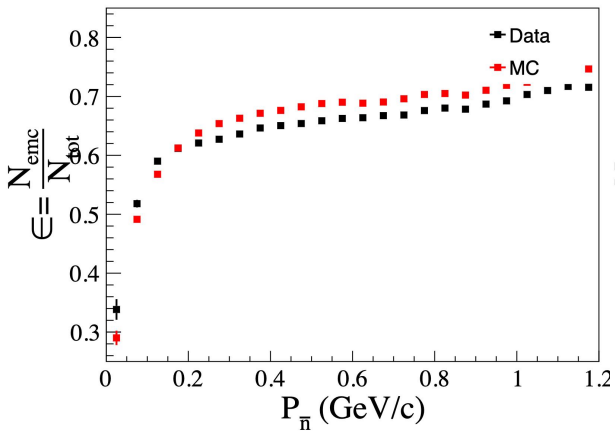
Rank	Variable	Variable Importance
1	eraw_gam_nbar	2.007e-01
2	qch2	1.530e-01
3	dtg	1.398e-01
4	qch1	1.381e-01
5	dtof	8.600e-02
6	qch3	4.991e-02
7	LastM_gam_nbar	4.980e-02
8	qch4	4.599e-02
9	erawoverpnbar	4.186e-02
10	eraw_tot_30d	3.489e-02
11	E33overEseed	2.363e-02
12	Nhit_gam_nbar	1.742e-02
13	E33overE55	1.636e-02
14	A20_gam_nbar	2.620e-03

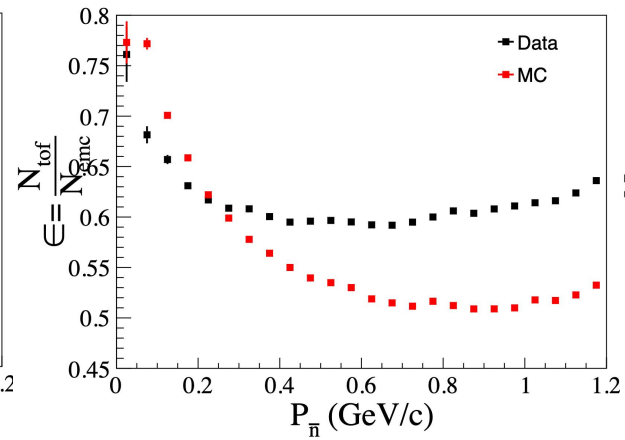
Improved TOF Reconstruction for Antineutron at BESIII:
Efficiency

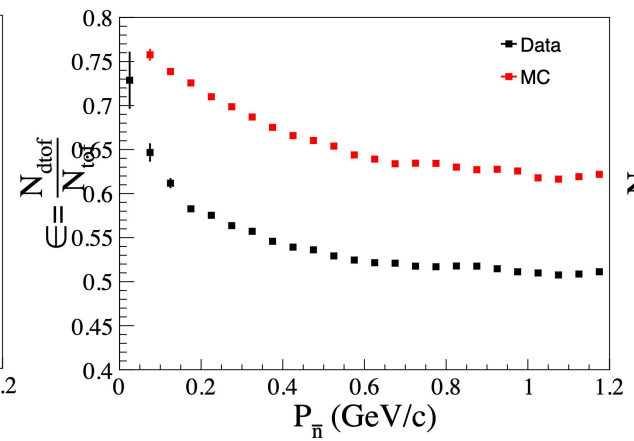
		Data Re. Eff. [%]	Data Abs. Eff. [%]	MC Re. Eff. [%]	MC Abs. Eff. [%]
EMC	$E_{\mathrm{emc}} > 0$	86.6	86.6	85.9	85.9
	$\Delta\theta_{\bar{n}\gamma} < 15°$	78.2	67.8	81.6	70.1
TOF	$t_{\mathrm{mea}} > 0$	60.6	41.1	52.6	36.9
TOF1 and TOF2	$tof1{,}2 > 0$	52.1	**21.4**	63.9	**23.6**
		Data [%] Ratio		**MC [%] Ratio/Purity/Eff.**	
BDTG Classification	Part1	49.6		49.5/75.1/84.3	
	Part2	21.9		18.3/70.0/48.0	
	Part3	28.5		32.2/69.9/77.2	
	Others	0		0	

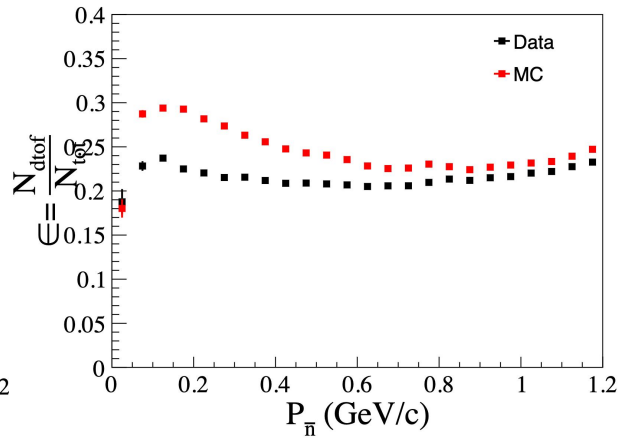
- ✓ Ratio: 经过BDT分类得到各个部分的比例。
- ✓ Purity: 经过BDT分类得到各个部分纯度。
- ✓ Efficiency: 第i部分正确分类的事例数/第i部分truth的事例数。

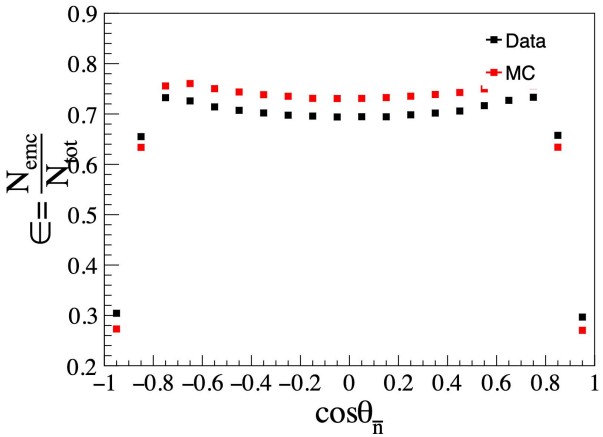
Efficiency

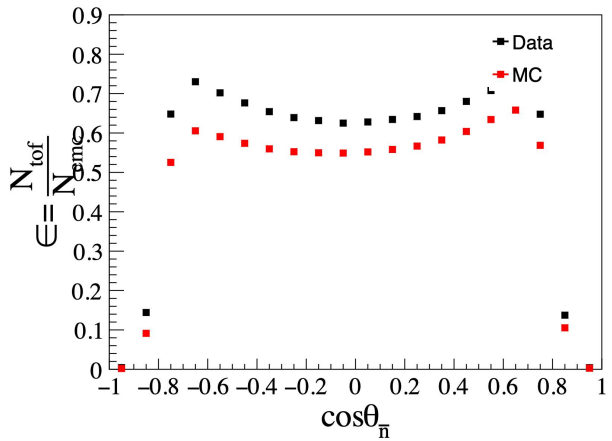

Data
MC
$\epsilon = \frac{N_{emc}}{N_{tot}}$
$P_{\bar{n}}$ (GeV/c)

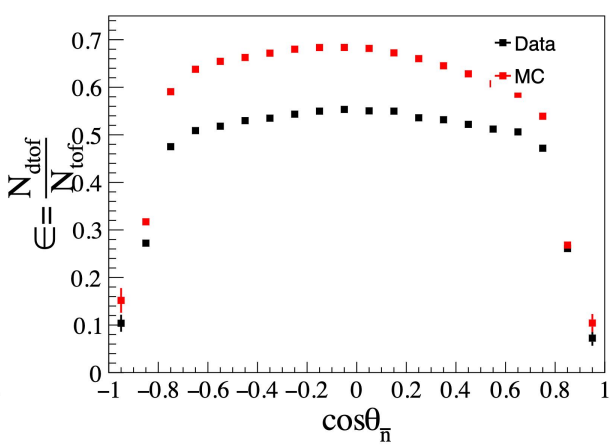

Data
MC
$\epsilon = \frac{N_{tof}}{N_{emc}}$
$P_{\bar{n}}$ (GeV/c)

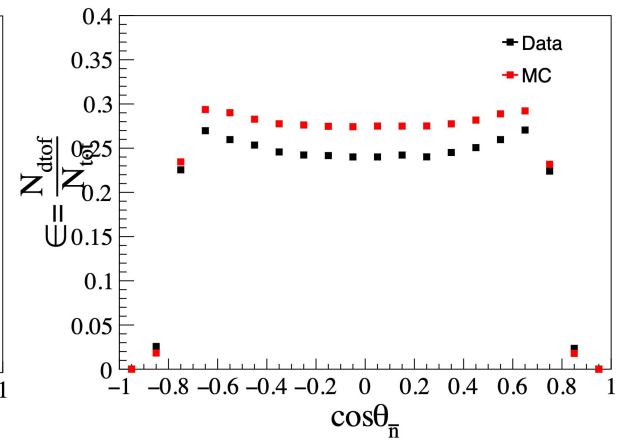

Data
MC
$\epsilon = \frac{N_{dtof}}{N_{tof}}$
$P_{\bar{n}}$ (GeV/c)


Data
MC
$\epsilon = \frac{N_{dtof}}{N_{tof}}$
$P_{\bar{n}}$ (GeV/c)


Data
MC
$\epsilon = \frac{N_{emc}}{N_{tot}}$
$\cos\theta_{\bar{n}}$


Data
MC
$\epsilon = \frac{N_{tof}}{N_{emc}}$
$\cos\theta_{\bar{n}}$


Data
MC
$\epsilon = \frac{N_{dtof}}{N_{tof}}$
$\cos\theta_{\bar{n}}$


Data
MC
$\epsilon = \frac{N_{dtof}}{N_{tof}}$
$\cos\theta_{\bar{n}}$